AWARD NUMBER: W81XWH-15-1-0621

TITLE: Brain Consequences of Spinal Cord Injury with and without Neuropathic Pain: Translating Animal Models of Neuroinflammation onto Human Neural Networks and Back

PRINCIPAL INVESTIGATOR: Nils Clas Linnman

CONTRACTING ORGANIZATION: Children's Hospital Corporation
Boston, MA 02115

REPORT DATE: October 2016

TYPE OF REPORT: Annual

PREPARED FOR: U.S. Army Medical Research and Materiel Command
Fort Detrick, Maryland 21702-5012

REPORT DOCUMENTATION PAGE

Form Approved
OMB No. 0704-0188

1. REPORT DATE	2. REPORT TYPE	3. DATES COVERED
October 2016	Annual	15 Sep 2015 - 14 Sep 2016

4. TITLE AND SUBTITLE

Brain Consequences of Spinal Cord Injury with and without Neuropathic Pain: Translating Animal Models of Neuroinflammation onto Human Neural Networks and Back

5a. CONTRACT NUMBER

5b. GRANT NUMBER

W81XWH-15-1-0621

5c. PROGRAM ELEMENT NUMBER

6. AUTHOR(S)

Nils Clas Linnman

Teng Yang

Lino Becerra

E-Mail:clas.linnman@childrens.harvard.edu

5d. PROJECT NUMBER

5e. TASK NUMBER

5f. WORK UNIT NUMBER

7. PERFORMING ORGANIZATION NAME(S) AND ADDRESS(ES)

Children's Hospital Corporation
Boston, MA 02115

8. PERFORMING ORGANIZATION REPORT NUMBER

9. SPONSORING / MONITORING AGENCY NAME(S) AND ADDRESS(ES)

U.S. Army Medical Research and Materiel Command
Fort Detrick, Maryland 21702-5012

10. SPONSOR/MONITOR'S ACRONYM(S)

11. SPONSOR/MONITOR'S REPORT NUMBER(S)

12. DISTRIBUTION / AVAILABILITY STATEMENT

Approved for Public Release; Distribution Unlimited

13. SUPPLEMENTARY NOTES

14. ABSTRACT

This project aims to investigate the consequence of spinal cord injury with regards to alterations in brain network function and expression of activated microglia, both human patients and in an animal model. During year one, we have: Obtained IRB and HRPO approval for the human studies, obtained IACUC and ACURO approval for the animal studies, refined the human study protocol and collected PET-MR data on healthy individuals and spinal cord injured subjects, developed the rodent imaging procedures including awake rat fMRI, collected pilot PET and MRI rat data, refined the spinal cord injury model. Human imaging data is of consistently high quality and is reliably collected, albeit with some concerns regarding patient recruitment being slower than anticipated. Animal imaging data is of sufficient quality, and efforts are underway to improve animal data collection. The animal spinal cord injury model has been refined. Data collection has been delayed due to regulatory procedures with regards to IACUC approvals, personnel training and personnel turnover.

15. SUBJECT TERMS

microglia, Positron Emission Tomography, functional Magnetic Resonance Imaging, translational medicine, spinal cord injury, rat, human

16. SECURITY CLASSIFICATION OF:			17. LIMITATION OF ABSTRACT	18. NUMBER OF PAGES	19a. NAME OF RESPONSIBLE PERSON
a. REPORT	b. ABSTRACT	c. THIS PAGE			USAMRMC
Unclassified	Unclassified	Unclassified	Unclassified	60	19b. TELEPHONE NUMBER *(include area code)*

Table of Contents

Page

1. INTRODUCTION

The goal of this project is to develop a translational framework where we define targets in SCI patients with and without neuropathic pain using a combination of clinical assessment, microglial Positron Emission Tomography (PET) and functional- structural- and diffusion- Magnetic Resonance Imaging (fMRI, MR, DTI). These measures of neural dysfunction and microglial activation are also be acquired in a rodent model of pre-SCI, subacute and chronic SCI and sham surgery. In the animal model, behavioral, sensorimotor function and histopathological/immunopathological staining data derived from tissue samples collected will be evaluated as the gold standard for neuronal and microglial alterations. Using this approach, imaging will serve as the "language of translation", allowing us to define human markers of disease and map them, via awake rodent imaging, onto detailed biological pathology. The direct comparisons between human and rat will define the utility of imaging to translate between bedside and bench. Detailed histology will further inform on the interpretation of imaging metrics.

2. KEYWORDS: microglia, positron emission tomography, magnetic resonance imaging, spinal cord injury, neuropathic pain, translational medicine, thalamus, sensory cortex, anterior cingulate, resting state functional connectivity, brain structure

3. ACCOMPLISHMENTS

Below we list the aims and sub-tasks from the statement of work on the grant, and the accomplishments in relation to the goals and timelines. Overall, the project is going well, with all the needed approvals in place and data collection methods piloted and finalized in the human and animal projects.

Specific Aim 1A: Define microglial activation as assessed by 11C-PBR28 PET in spinal cord injured patients with and without neuropathic pain.
Specific Aim 2A: Define brain structural, diffusion and functional network changes in the SCI populations.

Goal 1:Human PET-MR imaging of microglia and functional consequences in spinal cord injury with and without neuropathic pain.

Subtask 1: Obtaining IRB and HRPO approval for human studies (month 1-6)

Human IRB approval was obtained on 30/11/2015. USAMRMCORP HRPO of human protocol was approved on 14/12/2015.

Subtask 2: Recruitment, screening and scheduling of 1-3 patients per month (month 6-30)

Under the DoD mechanism, we will image twelve patients with SCI and neuropathic pain, and twelve patients with SCI but without neuropathic pain during the three-year project. In addition, the goal is to investigate twelve healthy subjects and another group of patients with spinal cord injury under a different funding mechanism (Wings for Life), thereby providing a sufficiently large sample. We have recruited a total of 29 subjects, whereof PET-MR data has been collected in 15 subjects (9 patients and 6 healthy controls). 6 of the recruited subjects were found ineligible, 3 subjects dropped out prior to scanning, and 5 are currently waiting to be scheduled. The investigated patients were

done under the Wings For Life funding mechanism, and we anticipate transitioning to DoD funding in months 12-24 according to plans.
Notably, patient recruitment has been slower than anticipated. This is likely due to multiple factors, including a) strict inclusion/exclusion criteria b) multiple co-morbidities in the SCI patient population, c) no direct medical benefit for SCI subjects volunteering in study, d) an approximate 10% loss of subjects due to incompatible genotyping, and e) a possible saturation of SCI studies in the Boston area.
To increase recruitment, we are actively engaging the SCI community via multiple channels: Volunteering at the Greater Boston Chapter for Spinal Cord Injury, contacts with physicians at Spaulding rehab hospital, and distributing recruitment material via the Boston University Health & Disabilities Research Institute, the 2016 Abilities expo in Boston, the Northeast passage (a recreational therapy non-profit in Durham New Hampshire), and to Adaptive Sports New England. With Dr. Dahlberg (post-doctoral fellow) joining the team in September 2016, we have increased our recruitment efforts substantially.

Subtask 3: PET-MR imaging, initial data quality control (month 6-30)

We perform data quality control continually with data collection, and have found the brain MR and PET data to be of consistently high quality. While the sample size is currently too small to perform a reliable statistical analysis of findings, we provide a sample of a sample of structural, resting state and PET data in two representative subjects:

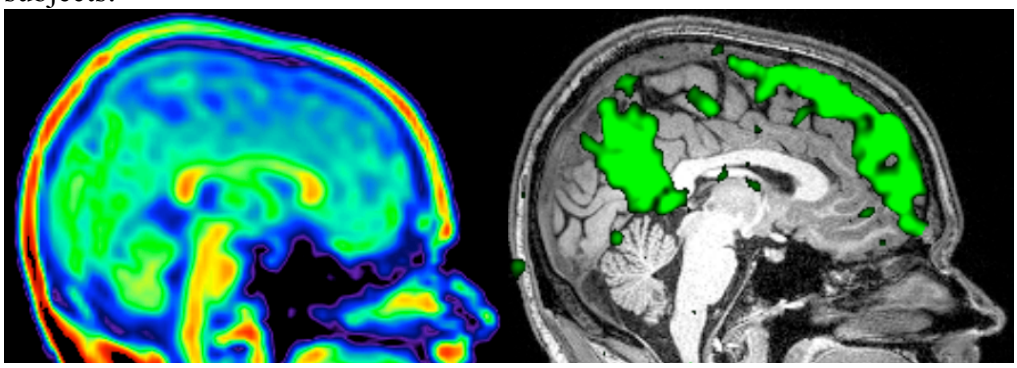

Figure 1: PBR28-PET (left), structural MRI (right) and "default mode" resting state network (FSL MELODIC independent component analysis indicated in green in right image) of a healthy male subject with no pain and no indication of neuroinflammation.

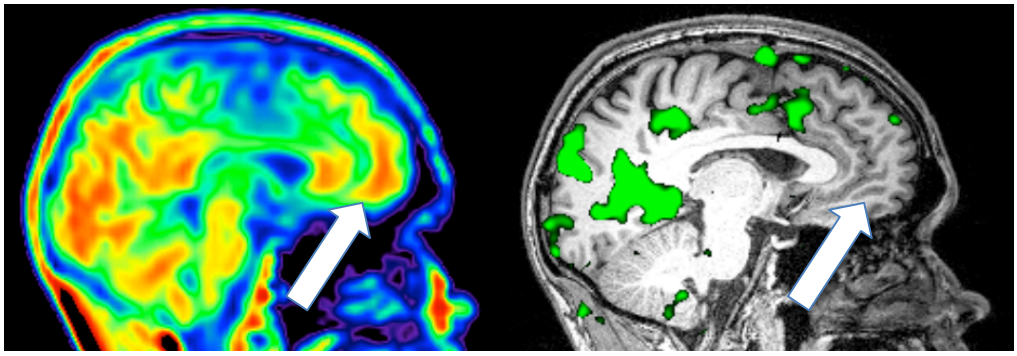

Figure 2: PBR28-PET (left), structural MRI (right) and potentially disrupted "default mode" resting state network in a patient with a C7-T1 ASIA-C spinal cord injury and neuropathic pain. The white arrow indicates potentially increased uptake of the PET-ligand, indicative of activated microglia and ongoing neuroinflammatory response with

associated lack of resting state network strength (independent component analysis in right image, in green).

Archiving of data: Data is continuously backed up on a dual RAID system and a physically separate cluster storage space.

Subtask 4: Data analysis

Group level data analysis will commence once we have adequate sized groups.

- Kinetic modeling and quantification of PBR28 uptake is ongoing
- Structural analysis of MRI data (Freesurfer segmentation and analysis) is ongoing
- Resting state fMRI analysis (Independent Component Analysis, Seed based connectivity, PET uptake driven connectivity modeling) is ongoing, see figure 1, 2.
- Diffusion data analysis (Fractional anisotrophy, tractography modeling, tractography statistical analysis) will commence in month 12-24
- Spine data analysis; segmentation, 11C- PBR28 quantification: This has been problematic to achieve as the absolute majority of SCI subjects have implanted steel or titanium rods, plates and screws to stabilize the injury. This greatly reduces our ability to image the lesion site on the PET-MR system, as metal implants introduce artifacts in the MR images and attenuate the PET data. We are currently experimenting with different sequences and analysis methods to provide PET-MR data also of the spine.

In addition to the above data analysis efforts, we have initiated a comprehensive review of the literature on brain alterations after spinal cord injury. The purpose of the review is to provide a) meta-analytical evidence for brain alterations in SCI, b) attempting to link SCI injury mechanisms to induced plasticity c) the impact of neuropathic pain on brain alterations in SCI, and d) the impact of emotional dysregulation on brain alterations in SCI.
The review is registered with PROSPERO (http://www.crd.york.ac.uk/PROSPERO/) (registration nr CRD42016032967) and is following Preferred Reporting Items for Systematic Reviews and Meta-Analyses (PRISMA) guidelines. 268 unique publications and records have been identified, whereof 75 full text articles have been assessed for eligibility. 60 studies will be included in a qualtiative synthesis of the current state of the field, and 6 studies can be included in a quantitative meta-analysis. The studies eligible for inclusion in the meta-analysis were analyzed using a new and improved method, signed differential mapping (SDM). SDM is a software based on previous meta-analytic methods such as multilevel kernel density analysis (MKDA) and activation likelihood estimation (ALE), which in addition can include both positive and negative results from the same coordinates, and use effect sizes to improve accuracy. Below are some of the preliminary data we intend to report in the review:

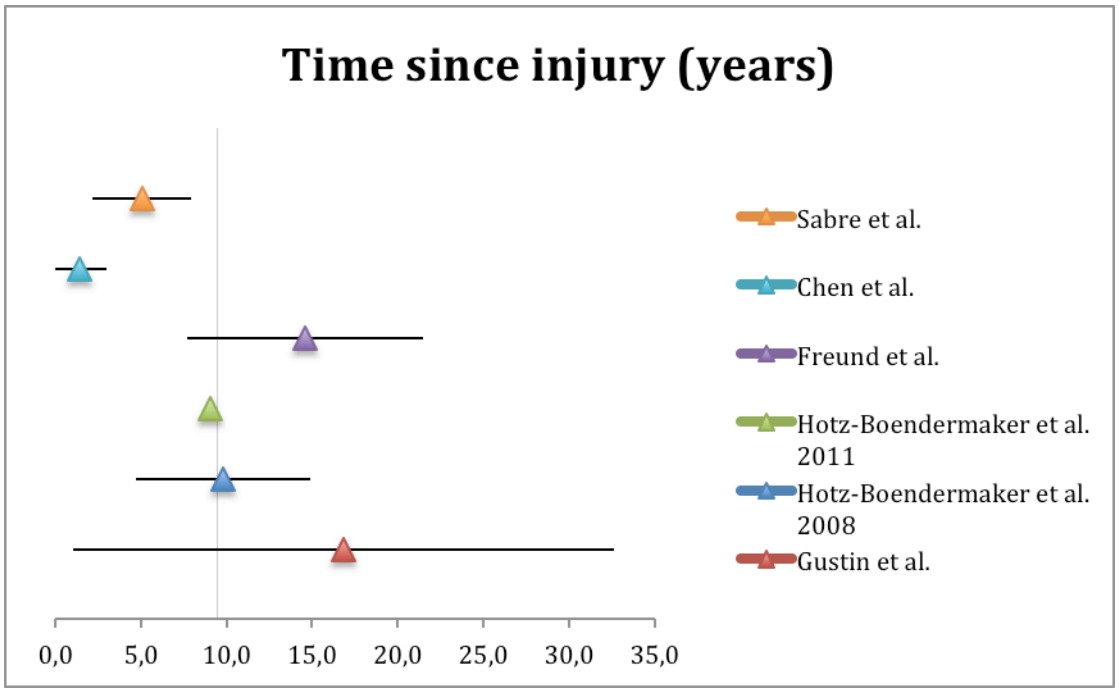

Figure 3: Average time since injury from each study included in the meta-analysis depicted forest plot displaying mean (years) ± standard deviation. Hotz-Boendermaker (2011) only listed average years since injury for the whole group, but specified a range between 2-20 years.

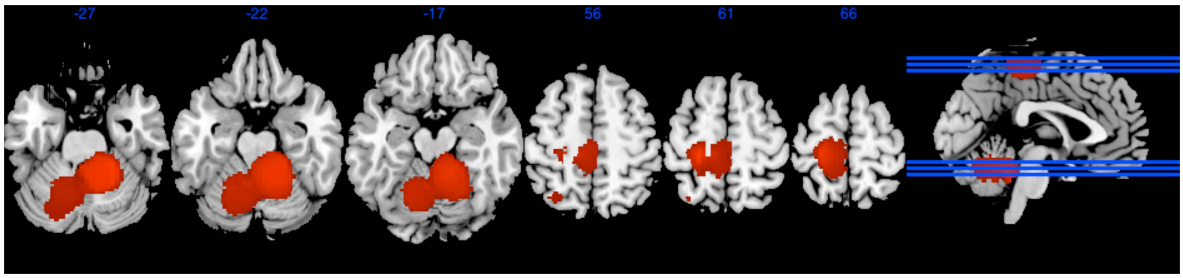

Figure 4. Regions commonly implicated in studies using attempted or imagined movement to evoke brain responses. The red regions indicate areas of significantly and consistently increased levels of activity in the SCI group compared to healthy controls.

We anticipate finalizing and publishing the review manuscript in year 2 of the project.

Specific aim 1B: Microglial activation as assessed by 11C-PBR28 PET in a Surgical Model of Moderate Static Compression SCI compared with non-operated controls.

Based on agreement initiated by Dr. Linnman, Project PI and concurred by Dr. Teng, Co-investigator, all rodent purchasing, surgery, and imaging will be performed at facilities of the Boston Children´s Hospital (BCH), respectively. For these endpoints Dr. Teng together with his new fellows and student have completed all IACUC training at BCH and registration in the past 1-3 months, which secured animal facility access and formal surgery observation evaluation by BCH's Animal Research Facility veterinary doctor and staff members. The basic science modeling component of the project is headed by Dr. Yang (Ted) Teng of the Brigham and Women's Hospital (BWH) that is located adjacent to BCH. Dr. Yang Teng, his newly added post-doctoral fellows Lei Wang and Dr.

Muhammad Abd-El-Barr, and newly added PhD student Hadi Hajiali, have completed occupational health screening, mandatory animal use training, and laboratory safety and radiation safety training at BCH. Dr. Teng and his team overcame time needed for member enrollment at BCH's multiple departments and for scheduling perfusion operation and aseptic surgery preparation observation evaluations; they are now ready to start the in vivo SCI modeling and behavioral data collection. During this time period the Teng Lab also successfully graduated its previous two postdoctoral fellows (Drs. Xiang Zeng and Liquan Wu) who moved onto a junior faculty position and clinical neurosurgery, respectively.

Major Task 2: Animal model and imaging

Subtask 1: Obtaining IACUC and ACURO approval for animal protocol (month 1-3)
Boston Children´s Hospital IACUC approved 01/21/2016
ACURO was approved on 04/18/2016 and communicated to us on 04/25/2016.

Subtask 2: Training Post doc II in Surgical Model of Moderate Static Compression (month 1-3).
Dr. Yang Teng and former post-doc II (Dr Xiang Zeng), and non-salaried fellow Dr. Liquan Wu and PhD student Hadi Haijal at Brigham and Women's Hospital received appointments at Boston Children's Hospital and achieved the required occupational health screening, animal use, lab safety and radiation safety training.

Dr. Teng and his new postdoctoral fellows Dr. Wang and Dr. Abd-El-Barr and PhD student Hadi Hajiali made extra efforts to complete all registration and occupational health and animal use training paper work. Dr. Teng and his team performed practice SCI modeling surgeries in his lab at BWH and VA Boston Healthcare System to fully standardize the quality of lower thoracic spinal cord injury model that will be used for the proposed imaging studies. These surgeries were done using the Teng Lab's own resources. Dr. Teng and his fellows and grad student further finalized and amended newly added anesthetic does suggested by the BCH veterinary team. The approved and updated protocol is now used by BCH for checking all preliminary bench work logistics and team setting up.

Subtask 3: microPET-CT imaging of SCI animals with Surgical Model of Moderate Static Compression (month 3-30)

We have defined and piloted the PET-imaging procedure in healthy rats, but have yet to produce a SCI animal for PET imaging. The PET data is of high quality, consistent with prior literature, see below

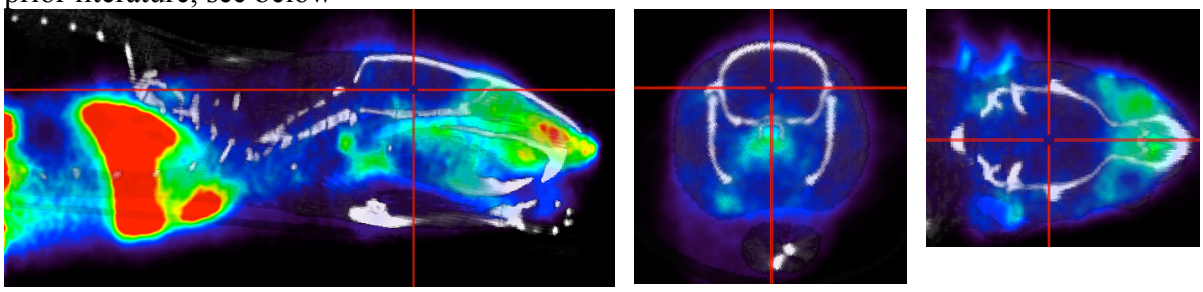

Figure 5: PBR28 uptake in a healthy rat, summary uptake over 60 minutes of imaging with an injected dose of 749 uCi. The image is overlaid with a CT. Notably, there is very

little uptake of the tracer in the brain (at crosshair) that is to be expected in non-injured animals. Further, the field of view of the PET-CT system will allow us to capture both brain and spine microglial response.

Milestone #1: Define preliminary translational capacity of PET imaging system (month 7-30)
C-11 PBR28 imaging has been achieved in both human and animals. The translational capacity between human and animal SCI microglial imaging remains to be defined.

Specific aim 2B: Brain structural, diffusion and functional network changes in the SCI model and control animals.
Major task 3: Awake rat fMRI
Subtask 1: Animal training (month 6-24)
Post-doctoral fellows Linda Dahlberg and Xian Zeng have been trained in the animal training and animal imaging protocols. Under a different project and IACUC protocol, rats have been investigated successfully.

Subtask 2: Control animal imaging (month 6-24)
No progress to report

Subtask 3: Pilot and define SCI animal imaging procedures (month 3-9)
We have refined our rat MRI-compatible holder to perform fMRI experiments proposed in this project, see figure 6, and now consider MR holder development completed. We also have finished testing fMRI sequences for this study. We use the following parameters (scanning was performed with a Bruker BioSpec 70/30USR 7T magnetic resonance imaging (MRI) scanner (Bruker, Billerica, MA)): A transmit-only volume coil with inner diameter of 85 mm in combination with a 4-channel phase array receive-only coil; A Bruker fastmap shimming program was performed to improve the homogeneity of the B0 field. High-resolution T2 weighted anatomical images were acquired with a fast-spin echo sequence (RARE; a field of view (FOV) = 20 mm x 20 mm, spatial resolution 0.078 mm x 0.078 mm, matrix = 256x256 voxels, slice thickness = 0.5 mm, slice gap = 0.1 mm, 34 slices, RARE factor 8, TR/TE= 4000/35 ms). Subsequently, a 10-min functional scan was obtained with co-centered single-shot BOLD resting-state fMRI time series using a gradient echo (GRE) with echo planar imaging (EPI) sequence (FOV= 20 mm x 20 mm, spatial resolution 0.313 mm x 0.313 mm, matrix = 64x64 voxels, slice thickness = 0.75 mm, slice gap = 0.15 mm, total 20 slices, TR/TE= 1000/37.323 ms, 600 volumes/animal).

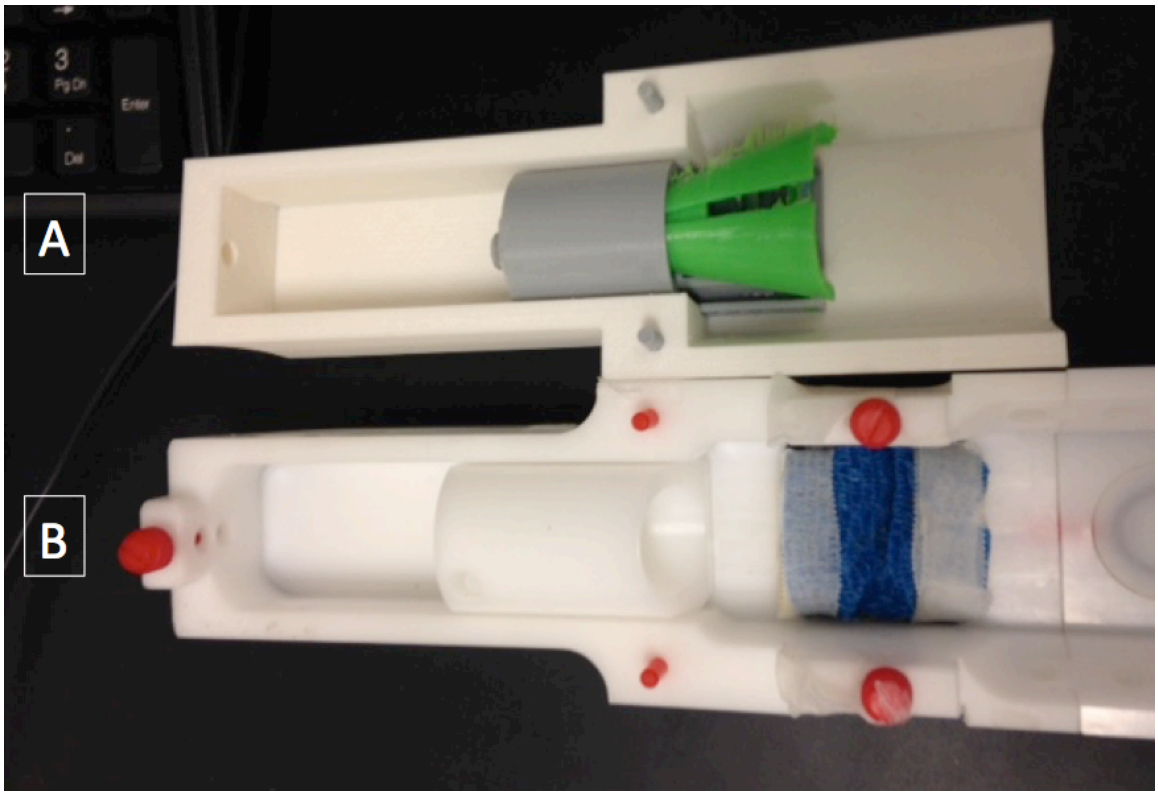

Figure 6: Holders for fMRI studies of rats. (A) depicts the new system that allows for awake fMRI experiments of rats for this project. (B) is the standard equipment provided with the MRI scanner.

We have now the ability to perform awake imaging studies that would eliminate anesthetic effects on brain signals. Our new MRI-compatible holder, in combination with animal training, minimized animal stress and head motion to allow for awake imaging. Figure 7, that indicates the absence of significant heat motion during scanning.. Furthermore, the equipment has been optimized to scan rats from 200-400 g in size, given that this project will last about 10 weeks and rats can grow significantly over that time, it was imperative to develop a system that will be able to scan animals in that weight range rather then utilizing different setups for different sizes.

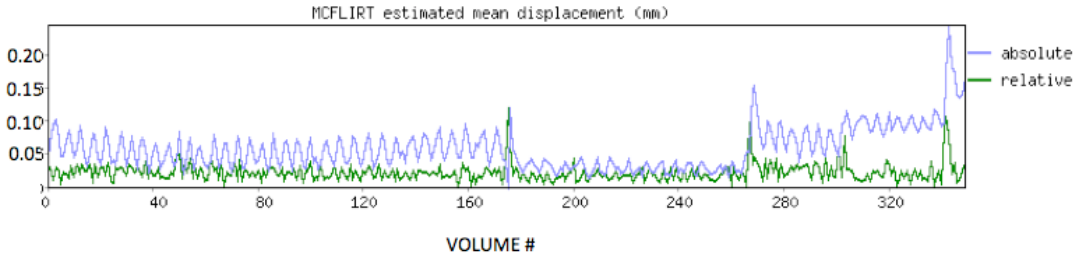

Figure 7: Absolute and relative (volume-to-volume) head displacement in an fMRI study of an awake rat. Displacement is less than half the in-plane resolution of the imaging. Such low displacement will not compromise acquired functional data.

We have performed independent component analysis (ICA) of the functional data to determine brain networks in the awake rat. We have properly identified several of the networks and an example is presented in Figure 8 in which the default mode network appears across 2 ICA components.

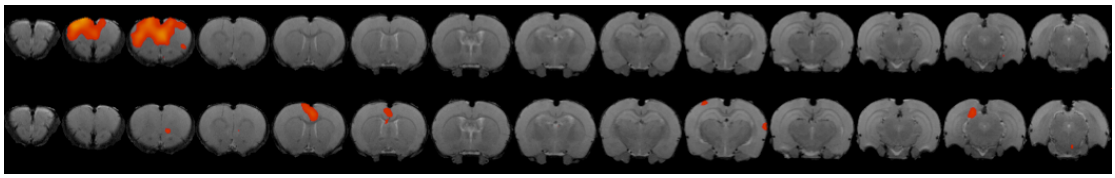

Figure 8. The default mode network appears resolved across two independent component analysis.

A new rat brain atlas was developed to facilitate analysis of brain structure and function.

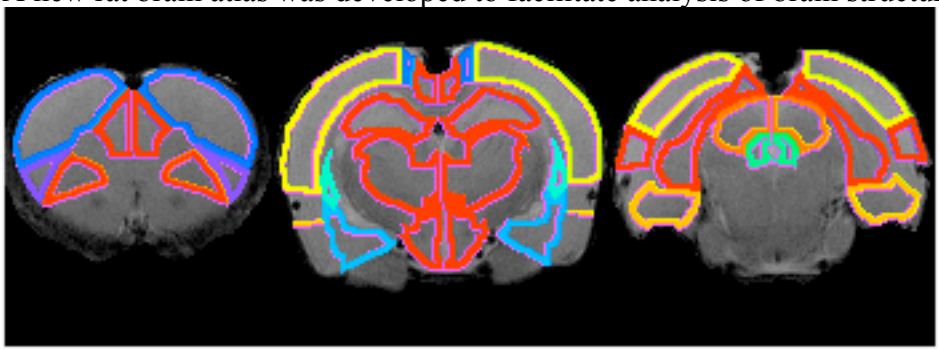

Figure 9. *Refined rodent atlas that corresponds better to our MR acquisition parameters.*

Subtask 4: Sub-acute and control animals (month 12-30)
No progress to report

Subtask 5: Chronic animal imaging (month 12-30)
No progress to report

Specific aim 3: Determine correlations between imaging findings and those of behavioral, sensorimotor function and histopathological / immunopathological staining results derived from tissue samples collected in animals from Aim 1B and 2B.

Major task 4: Histology and translation

Subtask 1: functional tests, histological, cellular and molecular assays, and data analyses

Dr. Teng has been working with Dr. Zeng and Dr. Wu for refining operation details regarding standardized moderate spinal cord compression injury of a rat model as per proposal submitted (i.e., 30 grams compression for 5 min at the lesion epicenter). They have also examined spinal cord sections that were produced by a previous study using a similar injury paradigm for obtaining information related to SCI-triggered inflammatory events. They have designs for how to refine the behavioral assays for chronic pain evaluation. Dr. Teng has also trained his new team of fellows and grad student for performing standard histopathology and immunohistochemistry to determine pathological outcomes such as neural inflammation that mainly underlies development of neuropathic pain. His team has obtained systematical knowledge and skill on performing correlative analysis between behavioral sensory disorders (e.g., hypersensitivity/pain-like behavior) and histological (e.g., sensory neural pathway), cellular (e.g., reactive gliosis, activated microglia), and molecular (e.g., pro-inflammatory molecules such as TNF-alpha) marker changes. Identification of these mediators or activators of post-SCI neuropathic pain will

provide therapeutic targets for developing clinical therapies to treat sensory disorder after traumatic SCI.

What opportunities for training and professional development has the project provided?

Dr. Clas Linnman, PI, attended the 2016 Wings For Life annual Scientific meeting in Salzburg, Austria on April 18-19 and presented preliminary findings.

Dr. Linda Dahlberg, post-doctoral fellow in the human project, attended the 2016 3rd international spinal cord injury and Neurotrauma Summer School, June 27th to July 1 in Hattingen, Germany.

Dr. Dahlberg has ben trained in awake rat functional MRI imaging

Dr. Dahlberg is continuously being trained in fMRI and PET imaging methods and data analysis

The first 9 months of this project has further scientific and professional training of two postdoctoral fellows at the Teng Lab – Dr. Xiang Zeng and Dr. Liquan Wu. They successfully graduated from the Teng lab per the initial training design of 1-4 years and have since become junior research faculty member and academic clinical neurosurgeon, respectively. Both previous fellows did excellent preparation work with Dr. Teng for finalize the animal use protocol design and documentation. Both obtained BCH veterinary team approval to perform formal surgical work for the project, which shows the quality of their experimental surgery training and post-care in the Teng Lab.

4. IMPACT

The long-term goal of this project is to develop a pipeline for translating promising therapeutics candidates in animal models of spinal cord injury onto the human condition. We currently focus on the role of microglial activity in SCI with neuropathic pain, but the general framework developed will be applicable to evaluate the translation potential of multiple agents. This approach can reduce the risk of running up blind alleys and putting patients at risk, allows using lower numbers of patients, and allows for a more informed approach in early clinical trials. While we do not yet have translational evidence for a shared microglial and functional response in the human and animal paradigms, the project is marching steadily towards that goal. We foresee multiple joint projects using the methods developed here in the near future.

The techniques that are being developed (microglial PET-MR in human, awake rat functional imaging) are likely to make an impact on multiple other disciplines, as neuroinflammatory responses are a key component of multiple neurological and neurodegenerative diseases.

Tehnology transfer

Nothing to Report.

Impact on society beyond science and technology?

Nothing to Report.

5. CHANGES/PROBLEMS

There are no changes to the protocol

Actual or anticipated problems or delays and actions or plans to resolve them

While we are on track with regards to animal imaging setup, we have yet to image an animal with spinal cord injury. This is due to a combination of factors; ACURO approval was obtained on April 25, 2016, i.e. 7 months after study initiation. Second, the spinal cord injury model was developed and implemented at Brigham and Women's Hospital, while PET and MR animal imaging is performed at Boston Children´s Hospital. As animals may not be operated on at the BWH and then transported to the BCH imaging facilities for quarantine reasons, the team of Dr Yang Teng and fellows have had to receive appointments and associated occupational health clearance, animal use orientation and training, and adaptations of procedures to the BCH regulatory environment.
The Teng Lab effectively went through team junior member change as per plan designed. The graduated members landed in higher career ground and new members already on track without encountering any work delay. Importantly, the new members will gain important research knowledge and skills through performing the proposed research work. Thus, the anticipated and effectively managed team transition additionally enhanced the project's overall impact. This process includes multiple instances of approvals needed.

There have been no significant changes in use or care of human subjects, no significant changes in use or care of vertebrate animals, and no significant changes in use of biohazards and/or select agents

6. PRODUCTS

Nothing to Report

Publications, conference papers, and presentations

Dr. Tengs laboratory has had two journal publications and one book chapter in part supported by the present grant.

1. Ropper AE, Zeng X, Haragopal H, Anderson JE, Aljuboori Z, Han I, Abd-El-Barr M, Lee HJ, Sidman RL, Snyder EY, Viapiano MS, Kim SU, Chi JH, **Teng YD**. Targeted Treatment of Experimental Spinal Cord Glioma With Dual Gene-Engineered Human Neural Stem Cells. Neurosurgery. 2016 Sep; 79(3):481-91.
2. Zeng X, Han I, Abd-El-Barr M, Aljuboori Z, Anderson JE, Chi JH, Zafonte RD, **Teng YD**. The Effects of Thermal Precondition on Oncogenic and Intraspinal Cord Growth Features of Human Glioma Cells. Cell Transplant. 2016 May 4. [E-pub ahead of print]

3. Teng YD, Zeng X, Han I, Anderson JE. Working with Stem Cells - Methodologies and Applications (Ulrich H and Negraes PD, Editors) Springer International Publishing, AG Switzerland. Chapter 18: Neural Stem Cells: Functional Multipotency and Spinal Cord Injury Research Protocols. pp. 311-329. 2016.

7. PARTICIPANTS & OTHER COLLABORATING ORGANIZATIONS

Name: Clas Linnman
Project role: PI
Researcher Identifier: 0000-0001-8449-894X
Nearest person month worked: 9, whereof 6 on the DoD mechanism
Funding Support: Dr. Linnman has received additional salary support (3 months) from the Promobila foundation

Contribution to project: Dr. Linnman has led the effort with regards to project planning, human IRB and animal IACUC approvals, setup and execution of PET-MR imaging of patients, setup and execution of PET imaging of rats, post-doctoral training, data quality control and analysis, and project reporting

Name: Yang Teng
Project role: Co-investigator
Researcher Identifier: 0000-0002-1257-4461
Nearest person month worked: 2
Funding Support: na
Contribution to project: Dr. Teng has contributed to IACUC approval, led the effort on development and refinement of the animal SCI model, post-doctoral training in animal surgery and care, and contributed to project reporting-

Name: Lino Becerra
Project role: Co-investigator
Researcher Identifier: 0000-0002-5840-1160
Nearest person month worked: 2
Funding Support: na
Contribution to project: Dr. Becerra has led the effort in developing the awake animal MRI holder, animal training procedures, MR imaging development, rodent MR data analysis and post-doctoral training in animal imaging. He has further contributed to IACUC approval and contributed to project reporting-

Name: David Borsook
Project role: Co-investigator
Researcher Identifier:
Nearest person months worked: 1
Funding Support: na
Contribution to project: Dr. Borsook has contributed to post-doctoral training and project management.

Name: Linda Solstrand Dahlberg
Project role: Post-doctoral fellow
Researcher Identifier: 0000-0002-1090-7138
Nearest person months worked: 4, whereof 0 on the DoD mechanism.
Funding Support: Dr Dahlberg has received salary support for work on the current project from Boston Children's Hospital internal funds, Promobilia foundation. Starting September 1, 2016, she is 100% dedicated to the current project.
Contribution to project: Dr. Dahlberg has contributed to human patient screening and recruitment, human PET-MR scanning, animal training, animal PET and MR imaging.

Name: Xiang Zeng
Project role: Post-doctoral fellow
Researcher Identifier: 0000-0003-4577-749X
Nearest person months worked: 10
Funding Support:
Contribution to project: Dr. Zeng has contributed to IACUC approval and development of animal SCI injury model.

What other organizations were involved as partners?
Organization Name: Brigham and Women's Hospital
Location of Organization: Boston, MA
Partner's contribution to the project: The spinal cord injury model was developed by Dr. Yang Teng at Brigham and Women's Hospital facilities, and his lab provides the expertise and personnel to perform this surgical model and post-operative care. Dr. Tengs lab is further responsible for behavioral testing and histological analysis of spinal cord and brain tissue.

9. APPENDICES

Publications that were, in part, supported by the present grant:

1. Ropper AE, Zeng X, Haragopal H, Anderson JE, Aljuboori Z, Han I, Abd-El-Barr M, Lee HJ, Sidman RL, Snyder EY, Viapiano MS, Kim SU, Chi JH, Teng YD. Targeted Treatment of Experimental Spinal Cord Glioma With Dual Gene-Engineered Human Neural Stem Cells. Neurosurgery. 2016 Sep; 79(3):481-91.

2. Zeng X, Han I, Abd-El-Barr M, Aljuboori Z, Anderson JE, Chi JH, Zafonte RD, Teng YD. The Effects of Thermal Precondition on Oncogenic and Intraspinal Cord Growth Features of Human Glioma Cells. Cell Transplant. 2016 May 4. [E-pub ahead of print]

Targeted Treatment of Experimental Spinal Cord Glioma With Dual Gene-Engineered Human Neural Stem Cells

Alexander E. Ropper, MD*‡§
Xiang Zeng, PhD, MD*‡§
Hariprakash Haragopal, BTech‡§
Jamie E. Anderson, BS‡§
Zaid Aljuboori, MD‡§
Inbo Han, MD‡§
Muhammad Abd-El-Barr, MD, PhD‡
Hong Jun Lee, PhD¶
Richard L. Sidman, MD‖
Evan Y. Snyder, MD, PhD#
Mariano S. Viapiano, PhD‡
Seung U. Kim, MD, PhD¶**
John H. Chi, MD, MPH‡
Yang D. Teng, PhD, MD‡§‡‡

‡Department of Neurosurgery, Brigham and Women's Hospital, Harvard Medical School, Boston, Massachusetts; §Division of SCI Research, Veterans Affairs Boston Healthcare System, Boston, Massachusetts; ¶Medical Research Institute, Chung-Ang University College of Medicine, Seoul, Korea; ‖Department of Neurology, Beth Israel Deaconess Medical Center, Harvard Medical School, Boston, Massachusetts; #Stem Cell Center, Sanford-Burnham Medical Research Institute, La Jolla, California; **Department of Medicine, University of British Columbia, Vancouver, BC, Canada; ‡‡Department of PM&R, Spaulding Rehabilitation Hospital, Harvard Medical School, Boston, Massachusetts

*These authors have contributed equally to this work.

Correspondence:
Yang D. Teng, PhD, MD,
Harvard Medical School,
No. 221 Longwood Avenue,
LM-111A,
Boston, MA 02115.
E-mail: yang_teng@hms.harvard.edu

Received, July 5, 2015.
Accepted, October 18, 2015.
Published Online, December 14, 2015.

BACKGROUND: There are currently no satisfactory treatments or experimental models showing autonomic dysfunction for intramedullary spinal cord gliomas (ISCG).

OBJECTIVE: To develop a rat model of ISCG and investigate whether genetically engineered human neural stem cells (F3.hNSCs) could be developed into effective therapies for ISCG.

METHODS: Immunodeficient/Rowett Nude rats received C6 implantation of G55 human glioblastoma cells (10K/each). F3.hNSCs engineered to express either cytosine deaminase gene only (i.e., F3.CD) or dual genes of CD and thymidine kinase (i.e., F3.CD-TK) converted benign 5-fluorocytosine and ganciclovir into oncolytic 5-fluorouracil and ganciclovir-triphosphate, respectively. ISCG rats received injection of F3.CD-TK, F3.CD, or F3.CD-TK debris near the tumor epicenter 7 days after G55 seeding, followed with 5-FC (500 mg/kg/5 mL) and ganciclovir administrations (25 mg/kg/1 mL/day × 5/each repeat, intraperitoneal injection). Per humane standards for animals, loss of weight-bearing stepping in the hindlimb was used to determine post-tumor survival. Also evaluated were autonomic functions and tumor growth rate in vivo.

RESULTS: ISCG rats with F3.CD-TK treatment survived significantly longer (37.5 ± 4.78 days) than those receiving F3.CD (21.5 ± 1.75 days) or F3.CD-TK debris (19.3 ± 0.85 days; n = 4/group; $P < .05$, median rank test), with significantly improved autonomic function and reduced tumor growth rate. F3.DC-TK cells migrated diffusively into ISCG clusters to mediate oncolytic effect.

CONCLUSION: Dual gene-engineered human neural stem cell regimen markedly prolonged survival in a rat model that emulates somatomotor and autonomic dysfunctions of human cervical ISCG. F3.CD-TK may provide a novel approach to treating clinical ISCG.

KEY WORDS: Autonomic dysfunction, Genetic engineering, Glioma, Neural stem cells, Spinal cord tumor, Targeted therapy

Neurosurgery 79:481–491, 2016 DOI: 10.1227/NEU.0000000000001174 www.neurosurgery-online.com

ABBREVIATIONS: 5FC, 5-fluorocytosine; **BBB,** Basso, Beattie, and Bresnahan; **CD,** cytosine deaminase; **DP,** diastolic blood pressure; **GCV,** ganciclovir; hNSCs, human neural stem cells; **ISCG,** intramedullary spinal cord gliomas; **MAP,** mean arterial blood pressure; **NSCs,** neural stem cells; **SP,** systolic blood pressure; **TK,** thymidine kinase

Supplemental digital content is available for this article. Direct URL citations appear in the printed text and are provided in the HTML and PDF versions of this article on the journal's Web site (www.neurosurgery-online.com).

Despite continued increase in clinical incidences, effective treatment for intramedullary spinal cord gliomas (ISCG) remains an unmet healthcare demand due to the tumors' poor response to conventional chemotherapy and radiation treatments.[1,2] The migratory and diffuse growth feature of glioma cells in the central nervous system often renders surgical treatment per se challenging and insufficient.[2] In the past decade, the unique capability of neural stem cells (NSCs) to migrate towards inflammatory pathology including tumor mass has been definitively appreciated.[3,4] Human NSCs

(hNSCs) administered in loci near primary tumors or systemically have been investigated for their ability to follow tumor cells in the brain.[5] The tumor trackability of NSCs has been attributed mainly to the chemotaxis impact of the tropic molecules secreted by tumor cells and the corresponding receptors expressed by NSCs.[3-6] After genetic engineering, hNSCs expressing cytosine deaminase (CD) and thymidine kinase (TK) can enzymatically convert nontoxic 5-fluorocytosine (5FC) and ganciclovir (GCV) into oncolytic 5-fluorouracil and GCV-triphosphate, respectively.[7,8] Both agents inhibit tumor growth by disrupting deoxyribonucleic acid elongation to trigger apoptosis.[7] We, therefore, hypothesized that the "bystander oncolytic effect" of the dual gene-engineered hNSCs may effectively treat ISCG utilizing their glioma trackability[3-7] and augmented therapeutic efficacy.[8]

To test our hypothesis, we evaluated the effect of the engineered hNSCs on killing glioma cells in vitro before examining their potency in a unique cervical ISCG model established by implantation of human G55 glioblastoma cells into the C6 spinal cord of immunodeficient/Rowett Nude rats. For the primary therapeutic parameters, we assessed evolvement of tumor-induced somatomotor and autonomic deficits and recorded overall survival in rats with ISCG.

METHODS

Culture of Human Glioma Cells and Genetically Engineered Human Neural Stem Cells

Human glioblastoma cell lines G55 and U87MG (both: World Health Organization grade IV astrocytomas; ATCC, Manassas, Virginia) were cultured with Dulbecco's Modified Eagle Medium (Life Technologies, Grand Island, New York) supplemented with 10% fetal bovine serum (Atlanta Biologicals, Flowery Branch, Georgia) and 1% penicillin/streptomycin solution (Life Technologies) in a 37°C and 5% CO2 incubator. Cells were regularly split with 0.25% Trypsin (Life Technologies) when they reached 80% confluency. F3.CD and F3.CD-TK cell lines were derived from the parental F3 hNSC line and maintained as per previously described protocols.[9,10] Please see the **Supplemental Digital Content** (http://links.lww.com/NEU/A825) for details regarding in vitro assays of a prodrug dose-response study for determining an optimal F3-hNSC and tumor cell ratio for the oncolytic effect.

Establishment of Intramedullary Spinal Cord Tumor Model

All in vivo experiments received approval from the Brigham and Women's Hospital and Harvard Medical School Institutional Animal Care and Use Committee. Immunodeficient female rats (Rowett Nude), age 8 to 9 weeks (body weight, 175-190 g; Charles River Laboratories, Wilmington, Massachusetts) were anesthetized by intraperitoneal injection of ketamine hydrochloride (75 mg/kg) and xylazine (10 mg/kg; Patterson Veterinary, Devens, Massachusetts). Rats were placed on a sterile surgery plate and their dorsal cervical regions were shaved and prepared with Betadine (Purdue Products L.P., Stamford, Connecticut) followed by 70% ethanol (Sigma, St. Louis, Missouri). A longitudinal incision (~2.0 cm) was made over the lower cervical region using a No. 10 surgical scalpel. The underlying fascia and muscle were dissected laterally and the C6 spinous process and lamina were removed with a rongeur. Next, the ligamentum flavum was resected, exposing the dura at the C6-7 intervertebral space. Using a No. 11 blade, the dura was opened to expose the spinal cord.

A custom glass micropipette was pulled by a P-97 Micropipette Puller (Sutter Instrument, Novato, California) using borosilicate capillary glass (CORNING 7740; Cat. #: BF100-50-7.5, Corning, New York). The shank outside and inside diameters were 1.00 and 0.50 mm, respectively, with a final tip length of ~5 to 7 mm and tip diameter of ~300 μm. The micropipette was loaded with phosphate-buffered saline (PBS) followed with cell or cell debris solution in each injection volume (i.e., 3 μL) (Figure 1) before the pipette was connected with a PBS-filled 50 μL Hamilton microsyringe (Hamilton, Reno, Nevada). The micropipette tip was inserted into the C6 spinal cord 2 mm beneath the dorsal pial surface. The tip was then retracted for 0.5 mm. The tumor cell suspension (10^4 in 3 μL PBS) was then injected slowly (3 μL/5 min) into the C6 level spinal cord parenchyma. The needle was kept in place after injection for another 5 minutes before removal

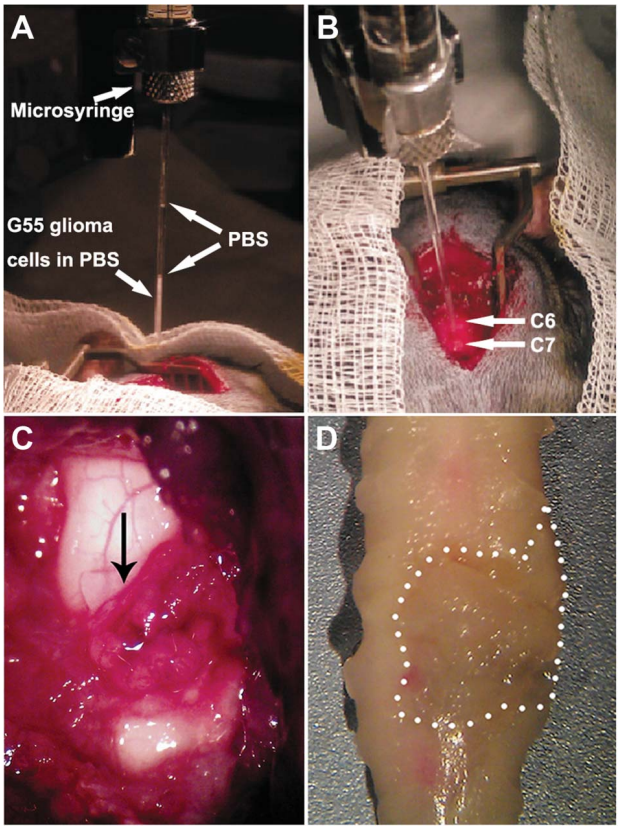

FIGURE 1. *Microinjection of G55 human glioma cells and general pathology of tumor growth in the spinal cord.* **A**, *tumor cells were loaded into a customized glass micropipette that was connected with a Hamilton microsyringe before injection.* **B**, *after laminectomy, 10K G55 cells in 3 μL PBS were slowly injected to the spinal cord.* **C**, *scale of tumor mass at 7 days after implantation at C6 (arrow; note: the appearance of the tumor mass was darker than the surrounding host tissue);* **D**, *scale of tumor mass (dotted line) after tissue fixation in a cell debris-treated spinal cord (ie, 21 days after G55 cell injection). PBS, phosphate-buffered saline.*

to prevent backflow of tumor cells. Surgical wounds were closed with staples.

Post-surgery care included pain management for 3 to 5 days with Buprenorphine (Patterson Veterinary, Devens, Massachusetts; 0.06 mg/kg, subcutaneous; twice a day), hydration (5 mL/day, subcutaneous, Lactated Ringer's solution, Baxter, Deerfield, Illinois), body temperature maintenance, and daily bedding material change. Rats were monitored for their bladder function: no rat showed micturition loss during the study period. No prophylactic antibiotics were used.

Study Design

To systematically test the effects of genetically engineered F3.NSCs on SGCs, we used a randomized block-design for the in vivo studies. Statistical power analysis was performed using SPSS 13.0 (Chicago, Illinois) after initial data acquisition. Based on the analysis, with 4 rats per group, there was ~95.5% possibility of detecting ≥42.7% of difference in mean survival time among F3.CD-TK-treated, F3.CD-treated, and F3 cell debris-treated groups. We therefore determined that a group size ≥4 would be adequate for analyzing the main outcome measures of the present study.

DiI Labeling of F3.hNSCs

F3.NSCs cells were pre-labeled 48 hours before transplantation by directly adding Cell Tracker CM-DiI (Life Technologies) to the culture medium with a final concentration of 2 μM (see more details in the **Supplemental Digital Content**, http://links.lww.com/NEU/A825).

Stem Cell Injection and Drug Administration

Seven days after tumor implantation, rats were re-anesthetized and partial laminectomies were performed one segment above and below the C6 tumor cell injection site. Rats with spinal cord glioma were injected with DiI pre-labeled F3.hNSCs (F3.CD-TK; F3.CD; or cell debris controls, n = 4/each; 1.5×10^6/10 μL/each site) at 1 mm rostral and 1 mm caudal to the visible tumor mass margins, using the aforementioned injection method. The incision was closed after hemostasis was achieved. Lastly, precursor drugs were administrated following the regimen below, starting 2 days after F3.hNSC injection:

1. F3.CD treatment: 5FC (500 mg/kg in 5 mL/day) and GCV (25 mg/kg in 1 mL/day), intraperitoneally for 5 consecutive days. Two days later the same regimen of 5 consecutive days of injection plus 2 days intermission was repeated until the rat met the termination criteria.
2. F3.CD-TK treatment: 5FC (500 mg/kg in 5 mL/day) and GCV (25 mg/kg in 1 mL/day) were administered intraperitoneally in the same 5 days on/2 days off format as previously described until termination criteria were met.
3. Control treatment: equivolume of debris of the same number of F3.CD-TK hNSCs plus repeated 5-FC and GCV administrations were given as per the method described in 2.

Evaluations of Somatomotor Abnormality and Longevity

Motor function and autonomic parameter assessments were carried out weekly. Hindlimb locomotor function was evaluated by the standard Basso, Beattie, and Bresnahan (BBB) scale.[11,12] Rats were euthanized based on the termination criteria of unilateral or bilateral hindlimb BBB score ≤9. Failure of such somatomotor function indicated a possibility for a rat to be not able to fully carry out self-care, especially for the current study where all rats with ISCG showed autonomic dysfunctions before their BBB score dropped to 9. Therefore, for meeting the high humane standard of animal warfare, BBB score ≤9 was used as a surrogate for post-tumor survival. After euthanasia, tissue was perfused and fixed with 4% paraformaldehyde. The spinal cords and the brains, together with other internal organs, were collected for histopathological and immunocytochemical analysis.

Autonomic Function Monitoring

Volume-pressure recording method for noninvasive blood pressure monitoring was adapted as previously described.[13] Blood pressure and heart rate were acquired by placing the tail-cuff device at the root of the tail. Ten successive data points were recorded to generate the average number for systolic blood pressure (SP), diastolic blood pressure (DP), and the heart rate for each measurement. Besides the 3 baseline data points, follow-up measurement was done weekly. When the BBB score dropped to 10 as the tumor progressed, measurement was done twice a week and once again before the termination. Mean arterial blood pressure (MAP) was computed based on an established formula of $MAP \approx DP + 1/3 \times (SP - DP)$.

For body temperature monitoring, a non-contact surface body temperature recording was carried out by using an infrared thermometer (TW2; ThermoWorks, Lindon, Utah) with an operating range from 0 to 50°C and a resolution of 0.1°C.

Respiratory function monitoring was carried out using our established method.[11,14,15] Briefly, baseline respiratory parameters were first established in conscious and free moving Rowett Nude rats.[11,15] Mean values for respiratory frequency (*f*), tidal volume (TV), minute ventilation (MV), inspiration time (IT), and expiration time (ET) were generated by the software through averaging the data from a 10-minute recording period. Besides 3 baseline data points, measurement was done on a weekly basis. When the BBB score dropped to 10 as the tumor progressed, measurement was done twice weekly and once again before termination (for more specifics, please see the **Supplemental Digital Content**, http://links.lww.com/NEU/A825).

Histopathological and Immunocytochemical Evaluations

The post-fixation spinal cord tissue was encased in optimal cutting temperature compound (Sakura Finetek USA, Inc, Torrance, California) and cryosectioned transversely at 20 μm thickness. Serial sections (1 of every 100 or 500 μm tissue) of the 1.0 cm spinal cord centered at the tumor epicenter were chosen for haematoxylin and eosin (Sigma) staining for general pathology analysis of tumor growth. In addition, one cross-section out of every 100 μm of tumor epicenter tissue was selected from each spinal cord for immunocytochemical detection of presence of F3.hNSCs in order to assess the tumor cell tracking capability and "bystander" oncolytic effect of the donor cells. For this purpose, human cell markers of human nuclei antigen (Millipore, Billerica, Massachusetts), human Nestin (Millipore) and cleaved caspase-3 (Cell Signaling Technology, Inc., Danvers, Massachusetts) were used to identify donor cells and apoptotic tumor cells, respectively. Slides were cover-slipped using mounting medium containing DAPI (Vector Labs, Burlingame, California) for confocal imaging of a Zeiss LSM1 confocal microscope equipped with Zeiss Zen 2011 software (Carl-Zeiss Microimaging, München, Germany). Histopathological data of tumor volume was analyzed by creating a computerized 3-dimensional reconstruction of the tumor mass based

on serial transverse pathologic slices stained with haematoxylin and eosin as described above (see details in the **Supplemental Digital Content**, http://links.lww.com/NEU/A825).

Data Analyses

Data were presented as mean ± standard deviation. One-way ANOVA (analysis of variance) with post-hoc Tukey honest significant differences test, Student's *t* test, and median rank test were used for statistical assessment using SPSS 13.0, with the statistical significance level set at $P < .05$.[11,14-17]

RESULTS

Our standardized approach (see Methods for details) (Figures 1A and 1B) resulted in robust G55 engraftment and growth. By 7 days post implantation, large exophytic tumor masses were clearly visible in all spinal cords implanted with G55 cells (Figures 1C and 1D). The in situ gross appearance of the tumor was darker than the surrounding non-tumor tissue of the spinal cord (Figure 1C; see post-fixation image in Figure 1D), which was caused by the tumor's denser cyto-angioarchitecture.[6]

In order to design an efficient pilot in vivo study, we first examined the response of G55 cells to the oncolytic impact of 5-fluorouracil and GCV-triphosphate converted from their precursor compounds of 5FC and GCV, respectively, by co-culturing G55 with F3.CD or F3.CD-TK. For the F3.CD and 5FC system, 5FC concentration was set at 270 μg/mL (2.1 mM), a medium dose in the range of 100 μg/mL to 500 μg/mL reported previously.[7,18,19] In the F3.CD-TK and 5FC + GCV setting, in addition to the same dose of 5FC, 3 μg/mL (12 μM) GCV was applied.[10] F3.CD plus 5FC and F3.CD-TK plus 5FC + GCV treatments showed significant tumor inhibition effect that reduced G55 cell growth rates by 60.78% ± 2.87% and 83.06% ± 1.38%, respectively, relative to vehicle-treated controls ($P < .05$; 3 × 3 wells/each dose/each assay; total: 9 assays; ANOVA with Tukey's post-hoc test) (Figure 2A). We additionally determined that 5FC or GCV treatment alone in the doses used had no harmful effect on the cultured G55 cells (data will be published separately).

All G55-injected rats developed pathologic behavioral signs resulting from tumor growth that manifested mainly as progressive loss of motor function in the hindlimbs. We used the BBB scale to evaluate the overall hindlimb locomotion capability. BBB score is a parametric ranking system that ranges from 0 to 21, where 0 indicates total paralysis and 21 a normal locomotor function. Importantly, a BBB score of 9 indicates a basic capability for a rat to do body weight-bearing stepping.[11,12] G55 growth in the cervical spinal cord model was aggressive, triggering the onset of the BBB score ≤9 (i.e., the primary criterion of termination) as early as 16 days post tumor cell injection in the control group receiving cell debris treatment (Figure 2B).

Importantly, ISCG rats receiving F3.CD-TK 7 days after G55 seeding and subsequent 5FC-GCV administration had significantly increased average survival (37.5 ± 9.4 days; group median: 39) relative to the F3.CD-treated (23.4 ± 6.3 days; group median: 24) and cell debris control (20.0 ± 3.2 days; group median: 23) groups ($P < .05$; n = 4/group; median rank test). The Kaplan-Meier curves demonstrated marked benefits of F3.CD-TK cell plus 5FC-GCV treatment on overall survival relative to the other 2 study groups (Figure 2C). In contrast to earlier reports of brain tumor data,[9,10] there was no significant impact of F3.CD regimen on the overall survival or in vivo tumor growth rate (see below) in our study. The data were corroborated by the fact that F3.CD plus 5FC alone showed discernibly lower potency than that of the F3.CD-TK in vitro (Figure 2A).

We next analyzed the speed of tumor growth via dividing the terminal volume of the tumor (unit: mm^3; derived from morphological data) by the post-tumor survival time of the rat. The speed of tumor growth was significantly slower in the F3.CD-TK-treated group (0.569 ± 0.035 mm^3/day) compared with rats that received either F3.CD (0.933 ± 0.015 mm^3/day) or F3.CD-TK debris (0.954 ± 0.013 mm^3/day; $P < .05$; n = 4/group; one-way ANOVA with post-hoc Tukey test). However, there was no significant difference in tumor growth rate between the F3.CD plus 5FC-GCV-treated group and the F3.CD-TK cell debris-injected controls (Figure 2D). We acknowledge that the tumor growth process might be very likely following a nonlinear course. The data, nevertheless, provided postmortem estimation for the tumor inhibitory impact of F3.CD-TK plus 5FC-GCV regimen.

Similar to most clinical cases of cervical spinal cord gliomas, rats with C6 ISCG showed progressive disturbance of autonomic function including abnormalities in blood pressure, body temperature, and respiratory pattern (Figure 3). Beginning at the third week after G55 cell seeding (i.e., 2 weeks after treatment), rats of the cell debris-injected control group, on average, showed significantly decreased SP. Their MAP reduced significantly at the terminal stage, compared with the pre-tumor baseline, although DP was slightly less affected (Figures 3A-3C). The MAP data suggested that the cervical tumor growth might have compromised tissue blood perfusion of the ISCG rats.[16] This extrapolation was corroborated by changes of body temperature in the same set of rats. We observed development of more severe hypothermia in the cell debris-injected control rats beginning in the third week after tumor cell injection (Figure 3D). Treatment with F3.CD-TK regimen significantly improved both MAP and body temperature maintenance in rats with ISCG, compared with cell debris-injected controls (Figure 3). Interestingly, F3.CD plus 5FC-GCV treatment also significantly benefitted body temperature maintenance (Figure 3).

Respiratory perturbation is a leading morbidity and mortality cause of cervical spinal cord pathology.[11,14,15,20] We observed respiratory pattern changes such as significantly decreased respiratory rate in the control ISCG rats, compared with the F3.CD-TK regimen-treated group (Figure 4A). The reduced respiratory rate in the control rats seems to be triggered by gradual weakness in the inhalation efficiency. Such deficiency was defined by the increased inhalation time during the breathing cycle, reflecting progressively reduced respiratory drive to the

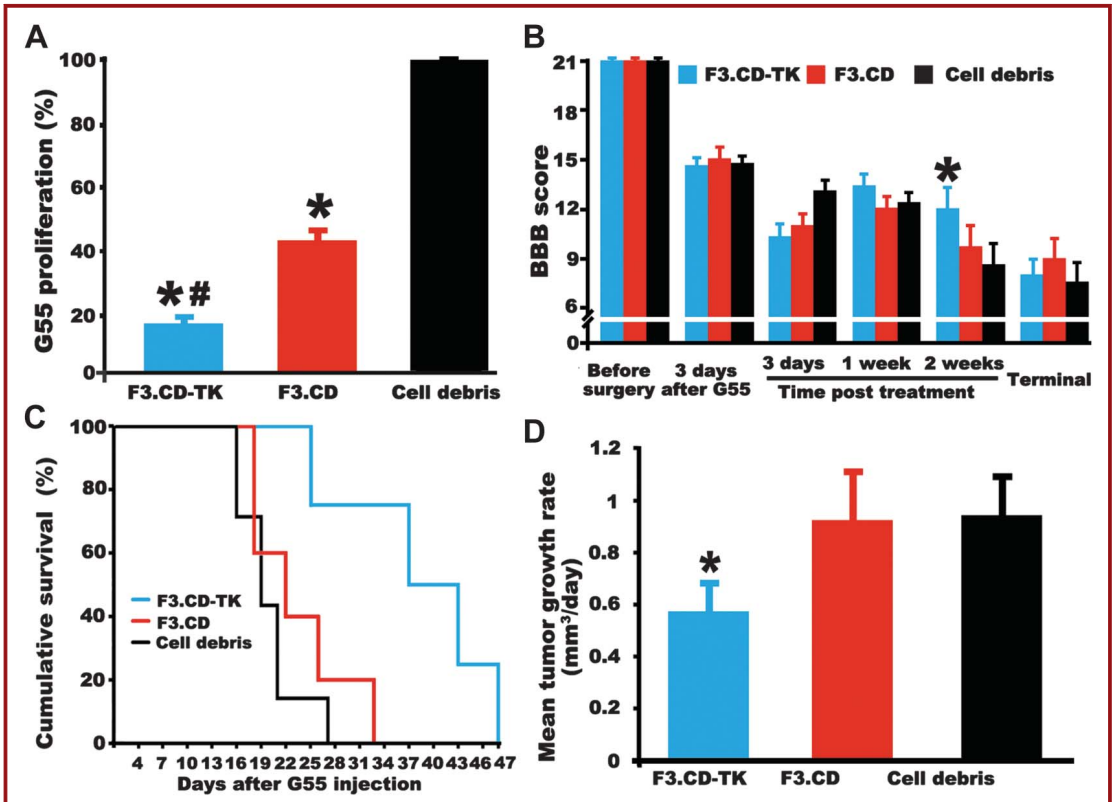

FIGURE 2. *Therapeutic effects of F3.NSCs in vitro and in vivo.* **A**, *in vitro cell culture study showed that F3.CD-TK plus 5FC and GCV regimen had significant higher oncolytic effect, inhibiting tumor cell proliferation by 83.06% ± 1.38%, compared with that of F3.CD-5FC treatment (60.78% ± 2.87%, relative to control rate of F3.CD-TK debris-treated G55 cells; n = 9; P < .05, ANOVA with Tukey's post-hoc test).* **B**, *C6 glioma rats showed progressive hindlimb functional deficit as assessed by Basso, Beattie, and Bresnahan (BBB) scoring. Rats with F3.CD-TK plus 5FC-GCV treatment had significantly reduced hindlimb functional loss starting 2 weeks after F3.CD-TK treatment, relative to the other 2 groups (P < .05, n = 4/group, ANOVA with Tukey's post-hoc test).* **C**, *Kaplan-Meier curves show overall survival estimates of rats with C6 gliomas after F3.CD-TK, F3.CD, or cell debris implantation plus 5FC or 5FC-GCV treatments, respectively (termination criterion: unilateral or bilateral BBB score ≤9). F3.CD-TK regimen significantly increased survival compared with other groups (P < .05, median rank test).* **D**, *F3.CD-TK regimen reduced tumor growth rate relative to that of either F3.CD group or cell debris-injected controls. *P < .05 when compared with cell debris group; #P < .05 (n = 4/group, ANOVA with Tukey's post-hoc test), compared with F3.CD-treated group.*

diaphragm, likely due to midcervical glioma compression to the phrenic motor neurons[14] (Figure 4B). However, there was no significant difference in the tidal volume (Figure 4C) and minute ventilation (Figure 4D) among the 3 groups at the end phase that was determined by loss of hindlimb capability of exerting consistent weight-bearing stepping.

Gross and histological examinations of the central nervous system and internal organs concluded that there was no ectopic or metastatic growth of G55 cells; however, we recognize that the relatively short study duration may have limited the detection capacity. We used 3-dimensional reconstruction analysis of the spinal cord microscopic images to investigate the tumor growth profile and F3.hNSC tumor infiltration scale. Our data revealed that all spinal cords with ISCG demonstrated similar cross section scales of tumor growth (Figure 5A) with longitudinal tumor ends reaching the C4 and C8 levels in most cases (Figure 5B). There were extensive penetrations of donor therapeutic cells into the tumor masses in the spinal cords of both F3.hNSC-treated groups (Figure 5A). Also confirmed by confocal microscopy were the drastically denser cell population inside the tumor mass relative to the surrounding host tissue (Figure 5C) and the presence of DiI-pre-labeled F3.hNSCs co-labeled by antibody against human nestin in the tumor zone (Figure 5D).

Immunocytochemical assays showed that F3.CD-TK regimen-treated spinal cords had significantly increased group average number of caspase-3 immunopositive apoptotic tumor cells that were diffusively surrounded by DiI-pre-labeled F3.CD-TK cells (Figure 6A); the F3.CD-5FC-GCV-treated group also had a significantly higher mean number of apoptotic tumor cells than that of the control spinal cords (Figure 6B). By contrast, there were only

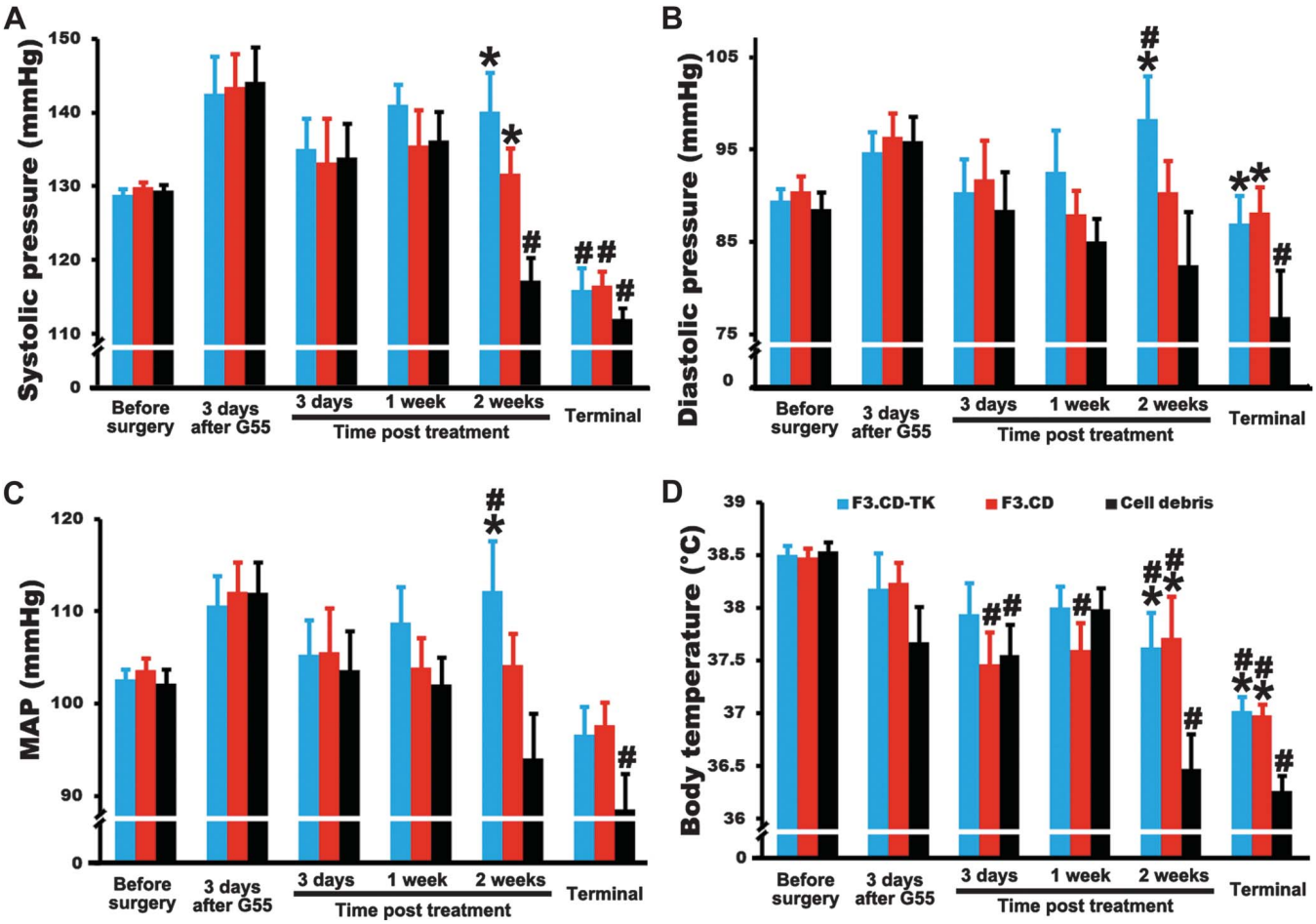

FIGURE 3. *Blood pressure and body temperature changes. C6 glioma rats showed a progressively decreasing trend of systolic and diastolic blood pressure, mean artery blood pressure (MAP), and body temperature levels. Compared with cell debris-treated group, F3.CD-TK cell regimen treatment significantly improved systolic blood pressure (A) and diastolic arterial blood pressure (B), starting 2 weeks after F3.hNSC injection, resulting in markedly improved MAP at the terminal stage (C). F3.CD regimen also improved systolic and diastolic blood pressure maintenance (A and B) compared with cell debris-injected control group. D, less body temperature decrease in F3.CD-TK or F3.CD group was also observed, relative to the controls. *P < .05 when compared with cell debris control group (n = 4); #P < .05 when compared with pre-surgery baseline data (n = 4/group, ANOVA with Tukey's post-hoc test).*

sporadic truncated caspase-3 positive apoptotic tumor cells in the cell debris-injected spinal cords (Figure 6C). The data suggested that the significantly improved survival and tumor growth reduction in the F3.CD-TK regimen-treated group likely resulted from the bystander oncolytic effect of the donor cell-converted chemotherapeutics; the combinatorial effect of 5-fluorouracil and GCV-triphosphate markedly suppressed tumor growth through inducing apoptotic death of G55 glioma cells in situ (Figure 6D).

DISCUSSION

Clinical incidence of ISCG is generally rare relative to that of brain glioblastomas; however, it could carry even poorer prognosis for many patients. Moreover, no targeted treatment has been established as either primary or adjuvant management for clinical spinal gliomas. In this pilot study, we designed and validated a rat model of cervical ISCG that showed reproducible and clinically relevant somatomotor and autonomic abnormalities of ISCG. In addition, using the model we have now demonstrated that CD-TK dual gene-engineered hNSCs significantly inhibited tumor growth and prolonged survival of rats with C6 ISCG by infiltrating tumor mass and locally converting benign precursor compounds into oncolytic drugs to trigger glioma cell apoptosis.

Despite potential risks, surgery is still considered a necessary option for many ISCG cases, because published studies showed that patient prognosis is significantly correlated with both pathological grade of the tumor and the presence of an intra-operative dissection plane.[21] However, for patients with World

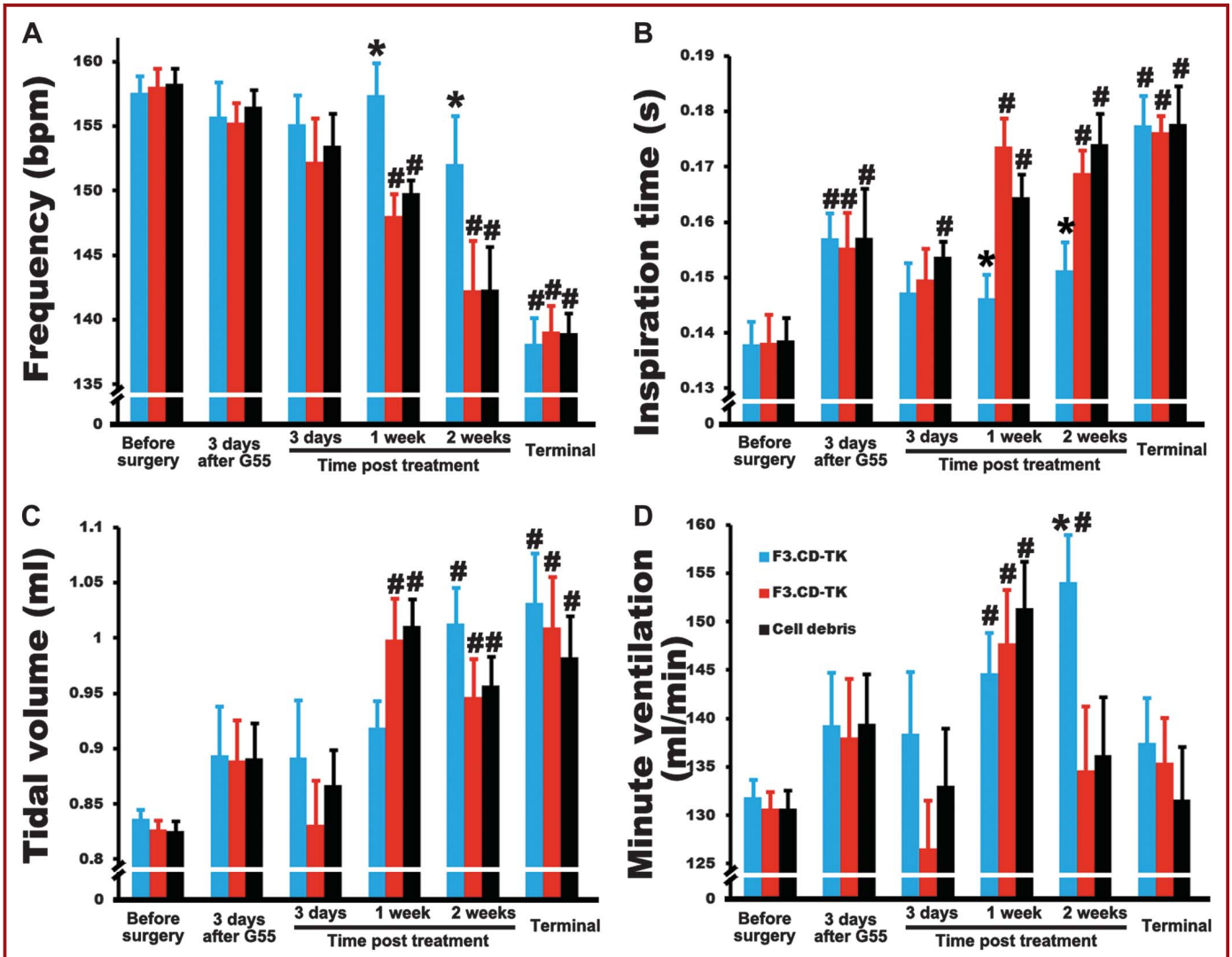

FIGURE 4. *Respiratory function changes. C6 glioma rats showed a progressive trend of decreased respiratory frequency (A) and increased of inspiration time (B), relative to their pre-tumor baseline respiration level. Treatment with F3.CD-TK cell implantation plus 5FC-GCV administration significantly improved inspiration time and respiratory frequency, starting 1 week after F3.NSCs implantation, compared with cell debris-injected control group (A and B). The combination of decreased respiratory frequency and increased inspiratory time helped to compensate for potential air volume loss (see tidal volume in C) due to breathing rate decreasing. This resulted in minute ventilation being maintained at levels not significantly reduced than pre-tumor baseline level prior to the terminal stage (D). *P < .05 when compared with cell debris control group (n = 4); #P < .05 when compared with pre-surgery baseline level (n = 4/group, ANOVA with Tukey's post-hoc test).*

Health Organization grade III or IV intramedullary spinal cord (ISC) tumors, about 61% of them showed further worsened functional status after surgical intervention, rendering gross total resection essentially not a feasible treatment option.[20] A large single center retrospective study found that the mean progression-free survival in patients with ISC malignant astrocytoma and glioblastoma was only 6.5 months, albeit the fact that all efforts were in place for providing most aggressive treatments available.[21] Furthermore, a long-term post-surgery follow-up of 202 patients with ISCG revealed that as many as 66% of the ependymoma patients, with 81% of them having received gross total resection treatment, reported no change in their clinical signs or symptoms.[20] Regarding noninvasive therapies, both chemotherapy and radiotherapy, given individually or combined, only showed very limited benefits in longevity improvement.[22-24] Taken together, the daunting reality of the dismal prognosis for high grade ISCG underscores the basic and translational science need for establishing new experimental models and developing efficacious targeted treatments.

Although there are dozens of preclinical studies and a few clinical trials involving the application of stem cell-based therapies for brain gliomas, there has been no study that investigated this

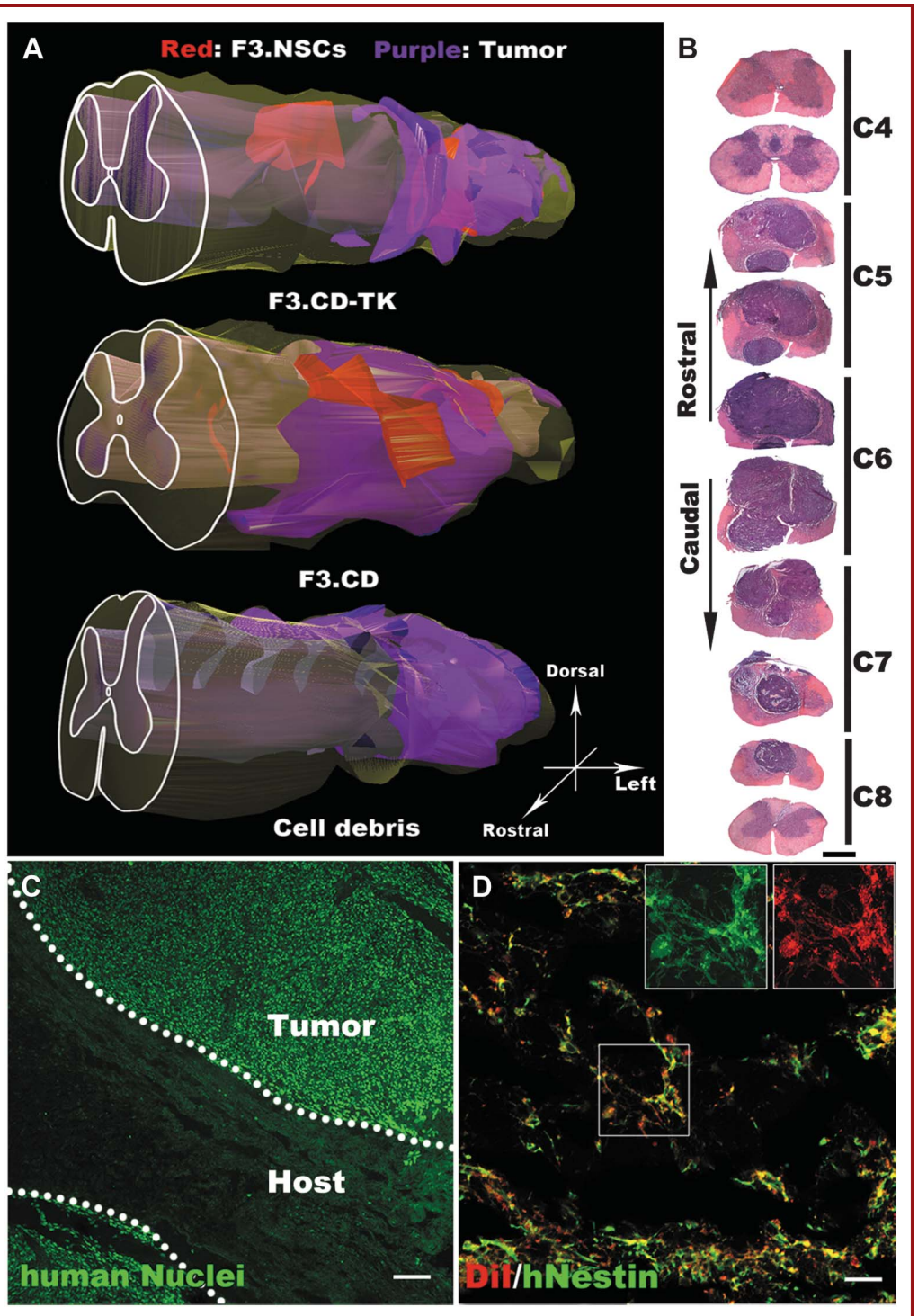

FIGURE 5. *Histopathology of the tumor-seeded spinal cord and immunocytology of tumor cells and implanted F3.NSCs in situ.* **A**, *images of 3-dimensional reconstruction of cervical glioma spinal cords of the 3 study groups.* **B**, *haematoxylin and eosin stain showed intraspinal cord distribution of G55 tumor masses. Intraspinal cord presence of densely populated G33 tumor cells is shown in (*C*). Red color-coded region in panel* **A** *indicates the penetration of the implanted F3.hNSCs, which migrated and infiltrated the tumor masses. The existence of F3.hNSCs was confirmed by detection of double signals of human Nestin and DiI-pre-labeling (*D*). Scale bars: 1 mm in* **B**, *100 μm in* **C**, *and 25 μm in* **D**.

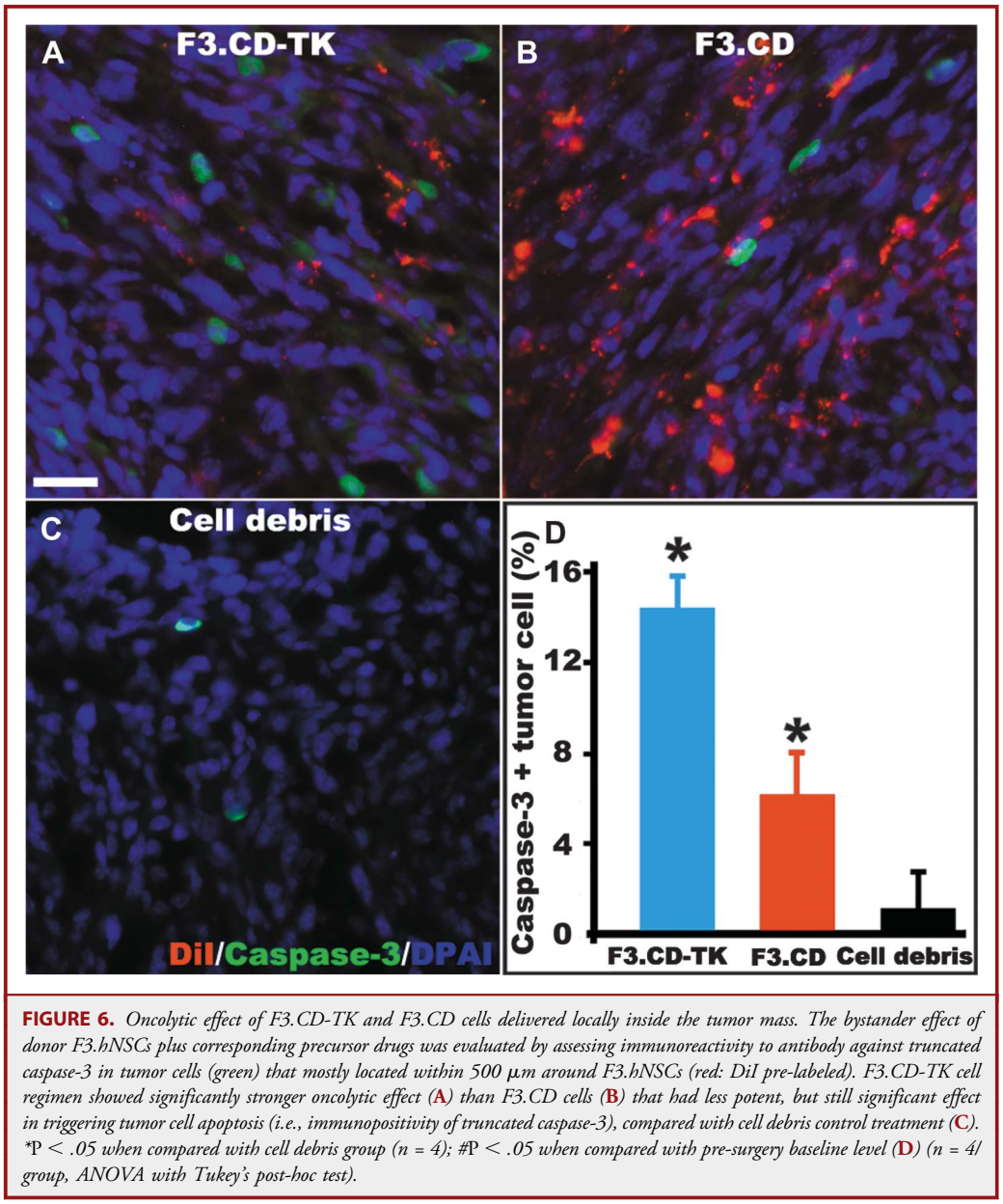

FIGURE 6. *Oncolytic effect of F3.CD-TK and F3.CD cells delivered locally inside the tumor mass. The bystander effect of donor F3.hNSCs plus corresponding precursor drugs was evaluated by assessing immunoreactivity to antibody against truncated caspase-3 in tumor cells (green) that mostly located within 500 μm around F3.hNSCs (red: DiI pre-labeled). F3.CD-TK cell regimen showed significantly stronger oncolytic effect (A) than F3.CD cells (B) that had less potent, but still significant effect in triggering tumor cell apoptosis (i.e., immunopositivity of truncated caspase-3), compared with cell debris control treatment (C). *P < .05 when compared with cell debris group (n = 4); #P < .05 when compared with pre-surgery baseline level (D) (n = 4/group, ANOVA with Tukey's post-hoc test).*

approach in ISCG.[5,7-10,25,26] We therefore systematically assessed the concept of gene directed enzyme prodrug therapy in our newly established model. There were 3 previously published articles on establishing a rat model of ISCG: all protocols showed reproducible intramedullary growth of glioma by directly injecting 9L gliosarcoma, 98L glioma, or glioblastoma multiforme neurosphere cells into the middle or lower thoracic spinal cord level.[27-29] The thoracic spinal cord tumor models reliably produced hindlimb locomotion deficits and offer feasibility of applying standard behavioral batteries (e.g., BBB locomotor scale[12]) to define the survival duration of the affected rats. The cervical spinal and cervicothoracic junction, regions housing enriched autonomic neural components, are more common sites for the multitude of growth of intramedullary tumors. Thus, autonomic abnormalities are often manifested by ISCG patients, which, sometimes, have life-threatening consequences.[30,31]

For patients with cervical spinal cord pathology (e.g., injury, tumor, etc.) research and medical attention has been routinely focused on maintaining the respiratory function.[32,33] In our model, the control ISCG rats showed significantly decreased respiratory rate underpinned with correspondingly increased inspiration time phase during the course of tumor growth (Figure 4). Overall, our data of respiratory changes corroborates with clinical observation for patients with cervical ISCG-related bilateral diaphragm weakness

who frequently demonstrate clinical signs of so-called "poor inspiratory effort" because about 70% of normal tidal volume in humans is attributable to the inspiratory work of the diaphragm.[34]

There was marked survival benefit in C6 ISCG rats treated with the F3.CD-TK plus 5FC-GCV regimen. This is the first stem cell-based multimodal therapy to significantly prolong longevity of ISCG rats by impeding glioma growth. The efficacy was not only better relative to the cell debris-implanted control group, but also better than the group treated with F3.CD regimen. Apparently, the failure for the single CD gene-engineered hNSCs, which showed efficacy in brain glioblastoma models, to exert discernible survival effect on rats with ISCG is novel experimental evidence corroborating the worsened tractability of cervical spinal cord malignant tumors. It suggests that a dual gene-engineered approach may help devise stem cell therapies with synergistic antitumor impact to treat high-grade ISCG. The dual gene synergy may be used as a component in well-designed combinatorial formulas for treating other types of conventionally intractable tumors, including hepatocellular carcinoma.[35] Our in vitro data indicates that a major advantage for the dual gene engineering strategy is its capacity to provide additionally augmented chemotherapeutic efficacy for disrupting deoxyribonucleic acid synthesis of high-grade glioma cells that respond very poorly to conventional treatments. Our ongoing studies are elucidating specific mechanisms underlying the synergistic effect, assessing ISCG-triggered somatosensory changes, and testing donor cell safety in naive animals.

CONCLUSION

This study has established an experimental model of cervical ISCG that manifests clinically relevant somatomotor and autonomic abnormalities. Using this system, we have developed a regimen of dual gene-engineered hNSCs plus prodrugs to efficaciously treat high-grade ISCG in rats. Since the US Food and Drug Administration recently approved the first clinical study evaluating a single CD gene-engineered hNSC-based therapy for recurrent high-grade gliomas in the brain (NCT01172964), we aim to deliver the first therapy for clinical ISCG using dual gene-engineered hNSCs to meet the healthcare demand for this category of devastating disorders[36,37] and to facilitate future therapeutic development for currently intractable metastatic diseases.

Disclosures

Portions of this study were presented at the 2015 American Association of Neurological Surgeons/Congress of Neurological Surgeons Joint Spine Section Meeting. The authors have no personal, financial, or institutional interest in any of the drugs, materials, or devices described in this article.

Author contributions: Y.D.T. and A.E.R. planned the first study and obtained the initial funding. X.Z., A.E.R., H.H., J.A., Z.A., I.H., and Y.D.T. did the experiments and generated data. H.J.L. and S.U.K provided genetically engineered stem cells. X.Z., A.E.R., and Y.D.T. summarized, analyzed, and plotted data, and drafted the manuscript. M.A., J.H.C., M.S.V., E.Y.S., and R.L.S. helped with study planning and progress. Y.D.T. initiated, supervised, and funded the study, and wrote and finalized the paper.

REFERENCES

1. Hsu S, Quattrone M, Ostrom Q, Ryken TC, Sloan AE, Barnholtz-Sloan JS. Incidence patterns for primary malignant spinal cord gliomas: a surveillance, epidemiology, and end results study. *J Neurosurg Spine.* 2011;14(6):742-747.
2. Kahn J, Loeffler JS, Niemierko A, Chiocca EA, Batchelor T, Chakravarti A. Long-term outcomes of patients with spinal cord gliomas treated by modern conformal radiation techniques. *Int J Radiat Oncol Biol Phys.* 2011;81(1):232-238.
3. Imitola J, Park KI, Teng YD, et al. Stem cells: cross-talk and developmental programs. *Philos Trans R Soc Lond B Biol Sci.* 2004;359(1445):823-837.
4. Imitola J, Raddassi K, Park KI, et al. Directed migration of neural stem cells to sites of CNS injury by the stromal cell-derived factor 1alpha/CXC chemokine receptor 4 pathway. *Proc Natl Acad Sci U S A.* 2004;101(52):18117-18122.
5. Aboody KS, Brown A, Rainov NG, et al. Neural stem cells display extensive tropism for pathology in adult brain: evidence from intracranial gliomas. *Proc Natl Acad Sci U S A.* 2000;97(23):12846-12851.
6. Schmidt NO, Przylecki W, Yang W, et al. Brain tumor tropism of transplanted human neural stem cells is induced by vascular endothelial growth factor. *Neoplasia.* 2005;7(6):623-629.
7. Kim JH, Kim JY, Kim SU, Cho KG. Therapeutic effect of genetically modified human neural stem cells encoding cytosine deaminase on experimental glioma. *Biochem Biophys Res Commun.* 2012;417(1):534-540.
8. Lee JY, Lee DH, Kim HA, et al. Double suicide gene therapy using human neural stem cells against glioblastoma: double safety measures. *J Neurooncol.* 2014;116(1):49-57.
9. Kim SK, Kim SU, Park IH, et al. Human neural stem cells target experimental intracranial medulloblastoma and deliver a therapeutic gene leading to tumor regression. *Clin Cancer Res.* 2006;12(18):5550-5556.
10. Wang C, Natsume A, Lee HJ, et al. Neural stem cell-based dual suicide gene delivery for metastatic brain tumors. *Cancer Gene Ther.* 2012;19(11):796-801.
11. Teng YD, Mocchetti I, Taveira-DaSilva AM, Gillis RA, Wrathall JR. Basic fibroblast growth factor increases long-term survival of spinal motor neurons and improves respiratory function after experimental spinal cord injury. *J Neurosci.* 1999;19(16):7037-7047.
12. Basso DM, Beattie MS, Bresnahan JC. A sensitive and reliable locomotor rating scale for open field testing in rats. *J Neurotrauma.* 1995;12(1):1-21.
13. Feng M, Whitesall S, Zhang Y, Beibel M, D'Alecy L, DiPetrillo K. Validation of volume-pressure recording tail-cuff blood pressure measurements. *Am J Hypertens.* 2008;21(12):1288-1291.
14. Choi H, Liao WL, Newton KM, et al. Respiratory abnormalities resulting from midcervical spinal cord injury and their reversal by serotonin 1A agonists in conscious rats. *J Neurosci.* 2005;25(18):4550-4559.
15. Teng YD, Bingaman M, Taveira-DaSilva AM, Pace PP, Gillis RA, Wrathall JR. Serotonin 1A receptor agonists reverse respiratory abnormalities in spinal cord-injured rats. *J Neurosci.* 2003;23(10):4182-4189.
16. Teng YD, Wrathall JR. Evaluation of cardiorespiratory parameters in rats after spinal cord trauma and treatment with NBQX, an antagonist of excitatory amino acid receptors. *Neurosci Lett.* 1996;209(1):5-8.
17. Teng YD, Choi H, Huang W, et al. Therapeutic effects of clenbuterol in a murine model of amyotrophic lateral sclerosis. *Neurosci Lett.* 2006;397(1-2):155-158.
18. Shimato S, Natsume A, Takeuchi H, et al. Human neural stem cells target and deliver therapeutic gene to experimental leptomeningeal medulloblastoma. *Gene Ther.* 2007;14(15):1132-1142.
19. Joo KM, Park IH, Shin JY, et al. Human neural stem cells can target and deliver therapeutic genes to breast cancer brain metastases. *Mol Ther.* 2009;17(3):570-575.
20. Raco A, Esposito V, Lenzi J, Piccirilli M, Delfini R, Cantore G. Long-term follow-up of intramedullary spinal cord tumors: a series of 202 cases. *Neurosurgery.* 2005;56(5):972-981; discussion 972-981.
21. Garces-Ambrossi GL, McGirt MJ, Mehta VA, et al. Factors associated with progression-free survival and long-term neurological outcome after resection of intramedullary spinal cord tumors: analysis of 101 consecutive cases. *J Neurosurg Spine.* 2009;11(5):591-599.
22. McGirt MJ, Goldstein IM, Chaichana KL, Tobias ME, Kothbauer KF, Jallo GI. Extent of surgical resection of malignant astrocytomas of the spinal cord: outcome analysis of 35 patients. *Neurosurgery.* 2008;63(1):55-60; discussion 60-61.
23. Santi M, Mena H, Wong K, Koeller K, Olsen C, Rushing EJ. Spinal cord malignant astrocytomas. Clinicopathologic features in 36 cases. *Cancer.* 2003;98(3):554-561.

24. Kim WH, Yoon SH, Kim CY, et al. Temozolomide for malignant primary spinal cord glioma: an experience of six cases and a literature review. *J Neurooncol.* 2011; 101(2):247-254.
25. Bexell D, Svensson A, Bengzon J. Stem cell-based therapy for malignant glioma. *Cancer Treat Rev.* 2013;39(4):358-365.
26. Aboody KS, Najbauer J, Metz MZ, et al. Neural stem cell-mediated enzyme/prodrug therapy for glioma: preclinical studies. *Sci Transl Med.* 2013;5(184):184ra159.
27. Caplan J, Pradilla G, Hdeib A, et al. A novel model of intramedullary spinal cord tumors in rats: functional progression and histopathological characterization. *Neurosurgery*. 2006;59(1):193-200; discussion 193-200.
28. Ren TJ, Wang ZC, Zhang YZ, Li D, Wang HY, Li ZZ. Establishment of intramedullary spinal cord glioma model in rats. *Chin Med J (Engl).* 2010;123(18): 2580-2585.
29. Hsu W, Siu IM, Pradilla G, Gokaslan ZL, Jallo GI, Gallia GL. Animal model of intramedullary spinal cord glioma using human glioblastoma multiforme neurospheres. *J Neurosurg Spine.* 2012;16(3):315-319.
30. Osborn JW, Taylor RF, Schramm LP. Chronic cervical spinal cord injury and autonomic hyperreflexia in rats. *Am J Physiol.* 1990;258(1 pt 2):R169-R174.
31. Furlan JC, Fehlings MG, Halliday W, Krassioukov AV. Autonomic dysreflexia associated with intramedullary astrocytoma of the spinal cord. *Lancet Oncol.* 2003; 4(9):574-575.
32. Teasell RW, Arnold JM, Krassioukov A, Delaney GA. Cardiovascular consequences of loss of supraspinal control of the sympathetic nervous system after spinal cord injury. *Arch Phys Med Rehabil.* 2000;81(4):506-516.
33. Krassioukov A, Warburton DE, Teasell R, Eng JJ. A systematic review of the management of autonomic dysreflexia after spinal cord injury. *Arch Phys Med Rehabil.* 2009;90(4):682-695.
34. McCool FD. Chapter 99. Diseases of the diaphragm, chest wall, pleura, and mediastinum. In: Cecil RLF, Goldman L, Schafer AI, eds. *Goldman's Cecil Medicine*. Philadelphia, PA: Elsevier Saunders; 2012:603.
35. Yi BR, Hwang KA, Kang NH, et al. Synergistic effects of genetically engineered stem cells expressing cytosine deaminase and interferon-beta via their tumor tropism to selectively target human hepatocarcinoma cells. *Cancer Gene Ther.* 2012;19(9):644-651.
36. Karikari IO, Nimjee SM, Hodges TR, et al. Impact of tumor histology on resectability and neurological outcome in primary intramedullary spinal cord tumors: a single-center experience with 102 patients. *Neurosurgery*. 2011;68(1): 188-197; discussion 197.
37. Snyder EY, Teng YD. Stem cells and spinal cord repair. *N Engl J Med.* 2012;366 (20):1940-1942.

Supplemental digital content *is available for this article. Direct URL citations appear in the printed text and are provided in the HTML and PDF versions of this article on the journal's Web site (www.neurosurgery-online.com).*

Acknowledgments

The work was mainly supported by a Brain Science Foundation grant to Drs Ropper and Teng, and by Teng Lab Research Fund. Other work at Teng Labs was supported by Center for Integration of Medicine and Innovative Technology-Department of Defense, Department of Defense, Veterans Affairs Research and Development. We thank the American Association of Neurological Surgeons/ Congress of Neurological Surgeons Section on Disorders of the Spine and Peripheral Nerves for the Mayfield Awards to Dr Ropper and the Larson Award to Dr Abd-El-Barr for their contributions to the project. The authors thank Dr Dou Yu for his help with Dr Ropper's preliminary surgical planning.

COMMENT

Teng et al state, "the daunting reality of the dismal prognosis for high grade ISCG (intramedullary spinal cord gliomas) underscores the basic and translational science need for establishing new experimental models and developing efficacious targeted treatments." In response to this need, they have designed an important experimental model of cervical spinal cord glioma for studying a novel gene directed enzyme pro-drug therapy. This strategy involves human neural stem cells engineered to enzymatically convert nontoxic chemotherapy precursors into oncolytic agents. The neural stem cells can be directly injected into the spinal cord, adjacent to the tumor locus. Then, systemically administered 5-fluorocytosine and ganciclovir, upon reaching the neural stem cells, are converted to 5-fluorouracil and ganciclovir-triphosphate for local tumor killing effect.

This small pilot study of 4 animals in each of 2 different treatment groups and 1 control group demonstrated significant benefit for those that underwent intraspinal injection of an F3.CD-TK cell line and subsequent intraperitoneal 5-fluorocytosine and ganciclovir administration. As with any pilot study, the promising results of this investigation lead to further intriguing questions. The investigators elected to use a human glioblastoma (World Health Organization grade IV) cell line for creating their tumor model. In humans, ependymomas and low-grade astrocytomas are more common intramedullary spinal tumors than glioblastomas. The impact of the higher-grade tumor used in this model may be most evident in the observed rapid disease progression, compared to what can be a more indolent course seen clinically. How this difference in tumor histology affects further study of experimental therapies, and eventual translation to patients with ependymomas and low-grade spinal cord gliomas remains to be seen.

The authors report survival as a primary endpoint. It deserves mention, however, that they defined survival based on a predetermined cutoff for hindlimb motor dysfunction. Per their study design, a hindlimb motor loss score low enough for the possibility to not fully carry out self-care was criteria for humane termination (hence, mortality). Therefore, the actual outcome measure was number of days post tumor implantation and therapy initiation before significant loss of hindlimb function—using a neurologic score as a surrogate for disease burden and progression. With a high-grade tumor and repeated direct spinal cord manipulation (tumor implantation, intraspinal stem cell injection), it may not be surprising that all animals ultimately demonstrated eventual hindlimb motor loss. As the investigators expand this pilot, it will be interesting to see how this therapy or perhaps a multi-modal strategy may affect other relevant oncologic measures such as tumor growth vs suppression or reduction.

Finally, transplantation of neural stem cells both experimentally and in humans is decades old. Yet, the possibility of neoplastic transformation of undifferentiated precursor cells remains a common concern, even though this has largely not been seen. The potential for the therapeutic neural stem cells in this model, adjacent to a high-grade tumor, to become de novo tumors will be an issue that will ultimately need to be addressed before future translation.

These questions and others are certain to be answered by this group as they carry this excellent work forward. Teng et al should be congratulated on an important advancement in an area of neurosurgery that has long deserved better scientific exploration, and ultimately a better treatment solution for affected individuals.

Daniel J. Hoh
Gainesville, Florida

DOI: 10.3727/096368916X691493

CT-1573 Provisionally Accepted 04/29/2016 for publication in

"Cell Transplantation"

The Effects of Thermal Precondition on Oncogenic and Intraspinal Cord Growth Features of Human Glioma Cells

Xiang Zeng[1,3], Inbo Han[1,3†], Muhammad Abd-El-Barr[1], Zaid Aljuboori[1,3], Jamie E. Anderson[1,3], John H. Chi[1], Ross D. Zafonte[2], Yang D. Teng[1,2,3*]

1. Department of Neurosurgery, Harvard Medical School/Brigham and Women's Hospital, Boston, MA, USA

2. Department of PM&R, Harvard Medical School/Spaulding Rehabilitation Hospital, Boston, MA, USA

3. Division of SCI Research, Veterans Affairs Boston Healthcare System, Boston, MA, USA

† Inbo Han's current affiliation is: Department of Neurosurgery, CHA Bundang Medical Center, Seongnam, South Korea (I.H.)

*Corresponding author: Y.D. Teng

Harvard Medical School - Neurosurgery

300 Longwood Avenue Honeywell 2, 02115 Boston, MA

Phone: 617-525-8676

Fax: 617-264-5216

E-address: yang_teng@hms.harvard.edu

Abstract

The adult rodent spinal cord presents an inhibitory environment for donor cell survival, impeding efficiency for xenograft-based modeling of gliomas. We postulated that mild thermal pre-condition may influence the fate of the implanted tumor cells. To test this hypothesis, high grade human astrocytoma G55 and U87 cells were cultured under 37°C and 38.5°C, to mimic regular experimental or core body temperature of rodents, respectively. *In vitro,* 38.5°C-conditioned cells, relative to 37°C, grew slightly faster. Comparing to U87, G55 demonstrated greater response to the temperature difference. Hyperthermal culture markedly increased production of HSP27 in most G55 but only promoted transient expression of cancer stem cell marker CD133 in a small cell subpopulation. We subsequently transplanted G55 cells following 37°C or 38.5°C culture into the C2 or T10 spinal cord of adult female immunodeficient rats (3 rats/each locus/per temperature; total: 12 rats). Systematical analyses revealed that 38.5°C-preconditioned G55 grew more malignantly at either C2 or T10 as determined by tumor size, outgrowth profile, resistance to bolus intratumor administration of 5-fluorouracil (0.1 micromole), and post-tumor survival ($P < 0.05$; n = 6/group). Therefore, thermal precondition of glioma cells may be an effective way to influence the *in vitro and in vivo oncological* contour of glioma cells. Future studies are needed for assessing potential oncogenic modifying effect of hyperthermia regimens on glioma cells.

Key words: spinal cord; spinal cord glioma; intramedullary tumor; glioma; glioblastoma; tumor stem cell; thermal stress; precondition; heat shock protein; cell doubling time

CT-1573 Cell Transplantation early e-pub; provisional acceptance 04/29/2016

Introduction

Glioblastoma multiforme (GBM) is the most malignant type of glioma (Grade IV classified by the World Health Organization) in the central nervous system (CNS). Despite the fact that primary tumors in the spinal cord, spinal nerve roots, and dura are rare compared to intracranial neoplasms, there is continued increase in clinical incidences (14). Most clinical studies reported that survival rate for intramedullary spinal cord gliomas (ISCG) is less than 24 months under maximum therapeutic intervenes (23,33). Since effective treatment remains an unmet medical demand due to the poor response to conventional surgical, pharmacological, and radiation managements, it is essential to devise effective and efficient modeling systems to investigate pathophysiological mechanisms and develop therapies for ISCG (30). However, to date, there have been only a few of experimental studies aiming to investigate spinal cord gliomas. The reality is partly caused by a generally inhibitory environment of the adult mammalian spinal cord, which limits donor cell engrafting (8,15,30). Therefore, capability to manipulate intraspinal cord engraftment of donor cells is a prerequisite for establishing xenograft-based ISCG models in mammalian species (15,19,30). Determination of proper *in vitro* culturing regimens (i.e., pre-conditioning) is an efficacious strategy to prime donor cells (10) and temperature plays a pivotal role in tailoring donor fate *in vivo* (29). It was reported that cardiac myoblasts with 39.0°C precondition increased their resistance to oxidant stress post implantation (37). Because core body temperature of the rat is normally between 36.5 – 38.5°C (36,38), we decided to test whether pre-conditioning human GBM cell lines under mild thermal environment of either 37.0°C or 38.5°C would affect the intraspinal cord oncological profile of glioma cells by

CT-1573 Cell Transplantation early e-pub; provisional acceptance 04/29/2016

assessing their proliferation and oncological features *in vitro* as well as growth potential and sensitivity to bolus treatment of 5-fluorouracil (5-FU), a prototype oncolytic drug *in vivo*.

Materials and Methods

Cell culture: Human glioblastoma cell lines investigated were U87MG (ATCC® HTB-14™; WHO grade IV astrocytoma; ATCC, Manassas, VA) and G55. G55 is a human glioblastoma cell line that was passaged *in vivo* through nude mice and re-established as a stable xenograft cell line. Dr. E.Y. Snyder of SBPDC kindly provided G55 cells that were initially donated by C. David James (Department of Neurological Surgery, UCSF) (16,43). G55 cells, growing in close comparability to U87 cells, possess signature genes and a VEGF profile similar to other Grades III-IV astrocytoma cells (20,31,43); however, because of their *in vivo* passaging-based establishment, G55 cells maintain more of the characteristics of primary human glioblastoma cell (16). G55 and U87MG were maintained with Dulbecco's Modified Eagle Medium (DMEM) (Life Technologies, Grand Island, NY) supplemented with 10% fetal bovine serum (FBS) (Atlanta Biologicals, Flowery Branch, GA) and 1% penicillin/streptomycin solution (Life Technologies) in a 37.0°C and 5% CO_2 incubator. Cells were regularly split with application of 0.25% Trypsin (Life Technologies) when they reached ~80% confluency. Due to the providers' established credibility, no additional authentication (e.g., DNA fingerprinting) was done for U87 and G55 in the present study.

Preconditioning GBM cells under 38.5°C setting: When G55 and U87 cells in 37.0°C and 5% CO_2 culturing reached 40-50% confluency, they were replaced into an incubator with an initial

CT-1573 Cell Transplantation early e-pub; provisional acceptance 04/29/2016

setting of 38.0°C and 5% CO2 and kept there for 24 hours; afterwards the incubator's ambient temperature was increased to 38.5°C. When the growing cells reached ~70% confluency (i.e., P0), they were split and passaged in a ratio of 1:5. Using the same cell propagation method, the G55 and U87 lines were maintained for two additional passages (i.e., P1 and P2). The total of 3 passages took about ~9 days for each group.

Calculation of cell doubling time (CDT): Each passage of cells under 38.5°C preconditioning and their 37.0°C counterparts were detached with Trypsin (Life Technologies) and prepared into single cell suspension. Cell numbers were counted by hemocytometer with trypan blue (Sigma-Aldrich®) stain being used as the exclusion standard for viability control. CDT was calculated based on the following formula (ATCC).

$$Cell\ Doubling\ Time\ (CDT) = T * ln2/ln(N_T/N_0)$$

N_0 = the number of the cells at the beginning of the incubation time

N_T = the number of cells at the end of the incubation duration (i.e., T)

T = the given duration (unit: hour, for the current study)

Note: T, the incubation duration, could be in any time unit.

Evaluation of HSP27 expression: Immunocytochemical stain (ICC) was used to evaluate the expression level of HSP27 (heat shock protein 27 kDa) in G55 cells. Briefly, P0 to P2 glioma cell groups post 37.0°C or 38.5°C preconditioning were seeded onto glass coverslips. When the confluency of the cells approached 80%, they were fixed with 2% paraformaldehyde (PFA). For the ICC, cell-seeded coverslips were washed with PBS containing Triton X-100 (0.3%) and

incubated in 5% (vol./vol.) normal donkey serum (Millipore, Billerica, MA) for 30 minutes. The incubation for the primary antibody against HSP27 (Catalogue No.: ADI-SAP-800; Enzo Life Sciences, Farmingdale, NY) took place under 4°C and overnight (i.e., ~12 hours). Afterwards, the specific secondary antibody (Jackson ImmunoResearch Laboratories Inc., West Grove, PA) was applied per specifications provided by the manufacturer. Cells were covered by using mounting medium containing DAPI (Vector Labs, Burlingame, CA) for fluorescent microscopic analysis (Carl Zeiss).

Evaluation of CD133 expression and caspase-3 activation: Briefly, P0 and P2 G55 cells following 37.0°C or 38.5°C conditioning were seeded on glass coverslips with an initial density of 7,500 cells/coverslip housed in 12-well culture plates (Falcon, BD Biosciences). After 72h, the cells reached 70-80% confluency before they were fixed with 2% PFA. Using the same preparation procedures, co-incubation with primary antibodies against CD133 (EMD Millipore, Billerica, MA), a cancer stem cell marker and cleaved caspase-3 (Cell Signaling Technology, Inc.), a cell apoptotic marker was carried out in 4°C overnight. Corresponding secondary antibody (Jackson ImmunoResearch Laboratories Inc.) were applied afterwards per specifications provided by the manufacturers. Mounting medium containing DAPI (Vector Labs) was used for coverslipping prior to laser confocal fluorescent microscopic analysis.

Quantification of fluorescent immunoreactivity of G55 cells: Percentage of immunopositive cells were quantified via dividing the total positive cell number by the total number of DAPI-labeled nuclei under each randomized 0.25 × 0.25 mm^2 microscopic fields. For ICC of HSP27, 3 fields for each coverslip and 3 coverslips per each culture condition were quantified (total: n =

CT-1573 Cell Transplantation early e-pub; provisional acceptance 04/29/2016

9). For quantifying CD133 and cleaved caspase-3 immunopositive cells, 5 fields for each coverslip and 3 coverslips per each culture condition were evaluated (total: n = 15). Therefore, the estimated total immunopositive cell number per coverslip = the total number of DAPI-labeled nuclei per coverslip x the % of immunopositive cells averaged from the 3 or 5 fields randomly sampled in each coverslip.

G55 xenograft in the rat spinal cord: (1) Surgery: Female immunodeficient rats (8-9 weeks old RNU, 175-190 grams of body weight; Charles River Laboratories, Wilmington, MA) were anesthetized with ketamine hydrochloride (75mg/kg) and xylazine (10 mg/kg; Patterson Veterinary, MA, USA) via intraperitoneal injections. Rats were placed on a heated sterile surgical plate and prepared for surgery. The C2 or T10 spinous process was identified followed by a longitudinal incision being made over it using a #10 surgical scalpel (Aspen™, Caledonia, MI). After tissue dissection laminectomy was made between C2-C3 or T10-T11 for each rat to expose the dorsal surface of the spinal cord. (2) Tumor cell implantation: Using a #11 sharp tip surgical blade (Aspen™) the dura was opened to access the spinal cord and a 26-gauge needle connected with a Hamilton™ microsyringe was inserted into the dorsal C2-C3 or T10-T11 spinal cord for a 2 mm dorsoventral penetration. The needle was then retracted 0.5 mm prior to microinjection of the P2 G55 cells (10^4 cells/3ml PBS) preconditioned under either 37.0°C or 38.5°C culture setting. The injection needle was kept inside the spinal cord for an additional 5 min before removal. After muscle and soft tissue closure with surgical suture (Ethicon 4-0, coated Vicryl suture, undyed braided), skin incision was stapled (Medline Industries, Inc. Mundelein, IL). The rats received the standard post-operation care (30). All experimental procedures were reviewed and approved by the Animal Care and Use Committee (IACUC) of

the Brigham and Women's Hospital and Harvard Medical School. (3) Evaluation of pathophysiological signs: Rats were monitored daily for general physical conditions including body weight, grooming frequency, hair and skin condition, facial porphyrin staining. Hindlimb functions were also tested daily and summarized weekly based on the Basso, Bresnahan and Beattie (BBB) scale as previously reported (6). For assessing the tumor's response to a bolus anti-tumor drug treatment (see below), rats were scheduled to receive a bolus administration of 5-fluorouracil (5-FU, Sigma-Aldrich®) when their BBB scores fell to ≤9 unilaterally (i.e., failure to carry out consistent weight-bearing locomotion), a physical sign indicating that they might not be able to fully carry out self-care and should be euthanatized (30).

Intratumor administration of 5-FU: When the BBB score of the hindlimb dropped to ≤9 resulting from ISCG growth, rats were anesthetized and prepared for surgery as described above. C2-C3 or T10-T11 laminectomy site was reopened in order to examine and access the tumor mass. A bolus microinjection of 10 µl of 5-FU (10 mM; dose: 0.1 micromoles) was done over 5 minutes via a needle inserted close to the center of the tumor mass. The needle was kept inside the tumor for another 2 minutes before removal. Rats were evaluated for general physical condition and hindlimb BBB score for another 72 hours before they were euthanatized by deep anesthesia with i.p. 90 mg/kg ketamine hydrochloride and 15 mg/kg xylazine (Patterson Veterinary) before systemic perfusion with 4% PFA. The spinal cord and the brain, together with other internal organs were collected for histopathological and ICC analyses.

Histopathological and ICC analyses: The post-fixation spinal cord tissue was embedded in OCT compound (Sakura Finetek) and cryosectioned transversely at 20 µm thickness. Serial

CT-1573 Cell Transplantation early e-pub; provisional acceptance 04/29/2016

sections (one of every 100 or 500 μm tissue) of the 1.0 cm spinal cord centered at the tumor epicenter were chosen for hematoxylin and eosin (H&E; Sigma-Aldrich®) staining for general histopathology analysis of tumor growth. In addition, one cross-section out of every 100 μm of tumor epicenter tissue was selected from each spinal cord for ICC evaluation. Histopathological data of tumor volume was analyzed by creating a computerized three-dimensional (3D) reconstruction of the tumor mass based on serial transverse pathologic slices stained with H&E as described recently (30).

Statistical analysis: Experimental data are expressed as mean ± SEM. Statistical significance was defined at the $P < 0.05$ level. Multi-group data were evaluated statistically by using one-way ANOVA (analysis of variance) with post-hoc Tukey HSD (honest significant differences) test. Outcomes of two-group studies were compared by paired or unpaired Student's *t* test. We used SPSS-based computation (SPSS 13.0; SPSS Inc.) for all data processing.

Results

Mild thermal precondition promoted growth of human GBM cells

Under regular tissue culture condition (i.e., 37.0°C and 5% CO_2), U87 cells and G55 cells had CDT at 21.55 ± 0.13 and 19.31 ± 0.11 hours, respectively (n = 9/group; **Figure 1**). For the purpose to avoid excessive stress due to sharply increased temperature, the two cell lines initially cultured in 37.0°C environment underwent a two-step protocol of thermal increment: they were first kept under 38.0°C for a 24-hours adaptation period before being exposed to 38.5°C for the continued culture. This design enabled the cells to have uninterrupted growth under different

CT-1573 Cell Transplantation early e-pub; provisional acceptance 04/29/2016

thermal settings without encountering any discernible levels of cell death. Under this protocol, P0 G55 and U87 manifested CDT of 18.80 ± 0.44 and 20.90 ± 0.42 hours, respectively (n = 9/group). In longer incubation time P1 and P2 G55 cells showed further augmented responses to exposure of 38.5°C ambient condition. Specifically, CDT of P2 G55 cells was further shortened to 17.40 ± 0.37 hours, significantly shorter than that of P2 U87 (i.e., 20.40 ± 0.32 hours; n = 9/group, $P < 0.05$, One-way ANOVA with Tukey HSD test; **Figure 1**). However, the overall CDT differences between the two temperature settings were limited. For example, P2 G55 CDT shortened about 1.91 hours (i.e., <10%) in average under 38.5°C comparing to 37.0°C. Correspondingly, there was only 16.60 ± 0.21 % increase in the total cell number per coverslip for 38.5°C-cultured P2 G55 cells vs. 37.0°C P0 G55 (n = 9/group). The result indicated that the designed thermal conditioning had no dramatic impact on glioma cell proliferation. In either group, no noticeable levels of cell death were present, suggesting that the thermally escalated cell proliferation was not caused by elimination of temperature-sensitive cell sub-populations. We therefore decided to focus on G55 cells for all the subsequent assays and analyses focusing on biological and oncological features of G55 cells (27,28).

Increased HSP27 expression in GBM cells following 38.5°C precondition

In order to determine whether there were any definitive cytological changes resulting from the thermal stress and partly underlying the 38.5°C exposure-triggered more robust cell division, ICC evaluation of heat shock protein 27 kDa (HSP27) expression was performed. HSP27 is a member of small HSP family with well-characterized functions of protein chaperone activity, thermotolerance, inhibition of apoptosis, and regulation of either normal or malignant cell

CT-1573 Cell Transplantation early e-pub; provisional acceptance 04/29/2016

growth (3,32). Under 37.0°C culture condition, only a fraction of P1 G55 cells synthesized HSP27 at detectible levels (i.e., 7.41 ± 2.23% of the cells counted, n = 9/group; **Figure 2**). However, when P1 G55 cells were cultured under 38.5°C, HSP27 expression level was significantly elevated (i.e., 72.52 ± 1.77% of the total cell growth field; n = 9, $P < 0.05$, One-way ANOVA with Tukey HSD test; **Figure 2**). Interestingly, the increase of HSP27 production in G55 cells following thermal exposure was partially a time dependent event. For example, after ~9 days of continued 38.5°C culture the HSP27 immunopositive percentage reduced to 60.33 ± 2.28% in P2 G55 cells, though remaining significantly higher than that of 37.0°C P1 G55 (n = 9, $P < 0.05$, One-way ANOVA with Tukey HSD test; **Figure 2**), suggesting that the cells were progressively acclimated to the 38.5°C culture condition by adjusting their essential biological processes such as growth rate (**Figure 1**), resilience to oxidant insults, and thermotolerance (e.g., upregulation of HSP27; 3,27,28,32).

Thermal culture transiently upregulated caner stem cell marker CD133 in a subpopulation of G55 cells that were apoptosis resistant: We next assessed the effect of thermal conditioning on the oncological feature of G55 cells by evaluating levels of cancer stem cell marker CD133 expression (11,44). In 37.0°C setting, 2.7 ± 0.16% of G55 cells expressed CD133. However, CD133 expression percentage of 38.5°C-cultured P0 G55 increased to 6.48 ± 0.36 but subsequently reduced to 3.96 ± 0.13 in P2 cells, both being significantly higher than 37.0°C setting ($P < 0.05$, n = 15/group, ANOVA with Tukey HSD test; **Figure 3A-D**). We then verified whether CD133-expressing G55 cells were more apoptosis resistant, a key oncological feature of cancer stem cells (5,11,44). Following 38.5°C culture, there was a significantly increased rate of apoptosis in G55 P0 cells but the degree of increase was very limited (i.e., 2.34 ± 0.13% vs. 1.64

CT-1573 Cell Transplantation early e-pub; provisional acceptance 04/29/2016

± 0.16% of 37.0°C; P < 0.05, n = 15/group, ANOVA with Tukey HSD test; **Figure 3E-H**) as detected by nuclear presence of cleaved caspase-3 for its known role in hyperthermotherapy-enhanced chemotherapy effect on human glioma cells (17). The apoptotic cell percentage decreased to 1.56 ± 0.10% in 38.5°C P2 cells that was insignificant comparing to 37.0°C control cells. In all the settings, immunoreactivity to cleaved caspase-3 was only observed in G55 cells that were negative for CD133 expression (**Figure 3E-G**; note: A-D respectively showed the same imaging fields in E-G).

***In vivo evaluation of* 38.5°C preconditioned G55 cells in the rat spinal cord for their oncological features**

As a pathophysiological sign of ISCG growth, rats showed gradually heightened impairment of the hindlimb locomotion and eventually lost the ability to sustain performing body weight-bearing stepping (i.e. BBB score ≤9). Therefore, per humane standards for animal care, the first daily detection on loss of weight-bearing stepping in the hindlimb was used to determine post-tumor survival duration (30). Because there was no significant statistical difference in the survival length between C2 (n = 3 x 2 temperature groups) versus T10 (n = 3 x 2 temperature groups) implantation of G55 cells (**Table 1**), the data of C2 and T10 groups were combined to assess whether there was any effect of 38.5°C or 37.0°C precondition on post-tumor survival. Indeed, immunodeficient rats with implantation of 38.5°C preconditioned G55 cells showed significantly shortened group mean survival time than the group received tumor cells preconditioned under 37.0°C (15.33 ± 0.67 days versus 18.33 ± 0.71 days, n = 6/group, P = 0.012, unpaired Student's t test). The outcome suggested that relative to 37.0°C exposure, G55

CT-1573 Cell Transplantation early e-pub; provisional acceptance 04/29/2016

cells post 38.5°C preconditioning augmented their malignancy in the rat spinal cord, resulting in more rapid deterioration of neural functions (**Figure 4; Table 1**).

We next examined if 38.5°C precondition also alternated the oncological resilience of G55 cells *in vivo*. This was done by evaluating the resistance degree of intraspinal cord G55 cells to a bolus intratumor administration of 5-FU given to the rat on the day when its BBB score dropped ≤9 (i.e., longevity endpoint; see Methods for more details). The drug 5-FU inhibits tumor growth by disrupting DNA elongation to trigger apoptosis (30). At 72 hours after 5-FU administration, rats with 38.5°C preconditioned G55 glioma demonstrated significantly poorer response to 5-FU chemotherapy compared to the 37.0°C group, as determined by further worsened mean BBB score, i.e., score difference between the first day of BBB ≤9 and that observed at 72 hours post 5-FU treatment. Rats with 38.5°C preconditioned G55 glioma had a group mean individual BBB score difference of 3.33 ± 0.42 (i.e., more than 3 points loss in average) versus -1.33 ± 0.91 (i.e., more than 1 point improvement) of the 37.0°C group (n = 6/group, $P = 0.001$, paired Student's t test). In fact, none of the rats of 38.5°C preconditioned G55 group showed motor function improvement following 5-FU administration; moreover, 5 out of the 6 rats had BBB scores that decreased ≥ 3 points. By sharp contrast, 4 out of the 6 rats received 37.0°C preconditioned G55 cells manifested motor functional improvement following bolus 5-FU treatment, showing the best BBB score improvement by 5 points (i.e., from 9 to 14; **Table 1**; **Figure 4**). The data indicated that mild thermal preconditioning could markedly influence the oncogenic features of human high grade glioma cells in the adult mammalian spinal cord (29).

Pathological features of intraspinal cord growth of 38.5°C preconditioned G55 cells

CT-1573 Cell Transplantation early e-pub; provisional acceptance 04/29/2016

There were strikingly different gross pathological profiles of gliomas derived from implantation of 38.5°C preconditioned G55 cells relative to those derived from 37.0°C cultured tumor cells (**Figure 5**). Among the 6 spinal cords that were injected with 38.5°C preconditioned G55 cells, 5 exhibited obvious tumor outgrowth disrupting the dorsal surface of the spinal cord (**Figure 5**: upper panel) whereas none of the glioma masses derived from G55 cells post 37.0°C preconditioning grew above the dorsal surface, leaving the spinal cord with a relatively smooth and largely intact dura membrane (**Figure 5**: lower panel). Furthermore, tumor size in rats received 37.0°C preconditioned G55 cells, in average, appeared smaller (**Figure 5**; **Table 1**). H&E (hematoxylin and eosin) staining histochemically validated the afore-mentioned conclusions (**Figure 5**). Therefore, 38.5°C precondition resulted in more robust outgrowth of G55 gliomas and higher resistance to chemotherapeutic effects that impede cell proliferation and viability (e.g., intratumor delivery of 5-FU; **Table 1**).

Discussion

The adult mammalian spinal cord, in general, presents a dormant and inhibitory environment for endogenous stem cells and donor cell engraftment. The feature sets up barriers not only for regenerative biology-based neural repair approaches but also for efforts to establish xenograft models of spinal cord disorders such as ISCG. In the current study, we observed that culture temperature difference exerted greater effect on G55 than U87 human glioma cells (e.g., CDT reduction). G55 cells preconditioned in 38.5°C, relative to 37°C, showed limited increase in proliferation and apoptosis rates; however, their HSP27 and CD133 expressions were markedly augmented. Comparing to sustainable levels of HSP27 increase, elevated expression of CD133 was transient in a G55 subpopulation. Importantly, 38.5°C culture enabled G55 cells to

CT-1573 Cell Transplantation early e-pub; provisional acceptance 04/29/2016

grow more robustly at either C2 or T10 spinal cord as determined by tumor size and growth profile, or resistance to anticancer efficacy of a bolus intratumor administration of 5-FU. We conclude that mild thermal pre-conditioning effectively influence the oncological features of human glioma cells *in vitro and in vivo*. Our data suggests that future studies should determine potential oncogenic modifying effect of hyperthermia regimens on glioma cells in order to devise efficacious ways to manipulate glioma cell fate.

Clinical incidence of ISCG is generally rare relative to that of brain glioblastomas, it, however, could carry even poorer prognosis for many patients. Moreover, no targeted treatment has been established as either primary or adjuvant treatments for clinical spinal gliomas. This reality is partly caused by difficulties encountered in endeavors trying to establish clinically relevant ISCG models (30). The temperature of the CNS of mammalian species, though conventionally ranged under "core body temperature", could be even ~1 °C higher than most of other internal organs due to its vigorous metabolic activity (1,2). Published work demonstrated that besides directly modifying interactions with neighboring cells and/or other environmental elements (24,34), the heat-shock pretreatment could be a practical method to influence cell fate in order to improve the success of the donor cell engraftment (7). We thereby designed and tested whether preculturing human high grade glioma cells under 37.0°C or 38.5°C ambient condition could impact the oncological features of U87 and G55, two glioma cell lines that may have different genetic and epigenetic profiles (43). It has been reported that moderate heat shock exposure (e.g., 43℃ for 1 or 2 hours), clinically applied to tumor-brain border-zone, caused cancer cell acute autophagy and cell cycle arrest, but did not induce apparent tumor cell apoptosis (21,46). However, to date, very limited attention has been given to the effect of even milder temperature elevation (e.g., 38.5℃ used in the current study) on the oncological features

CT-1573 Cell Transplantation early e-pub; provisional acceptance 04/29/2016

of human glioma cells. Our data shows that whereas the two-step incremental exposure from 38.0℃ to 38.5℃ culture slightly reduced CDT in U87 and G55, it discernibly impacted expression paradigms of HSP27 and cancer stem cell marker CD133 in G55 cells. Furthermore, our mild hyperthermia regimen heightened engraftment, growth, and viability resilience of G55 in the adult rat spinal cord. At least part of the precondition-triggered changes could be underlined by 38.5℃-induced upregulation of HSP27. As a chaperone protein responding to heat stress, HSP27 is one of the most widely studied heat shock proteins in oncology since it plays a major role in inhibiting extrinsic and intrinsic cell death signaling pathways to reduce apoptosis (4,9). HSP27 is also related to the state of tumor growth and to the aggressive state of tumor cells (13,32,41,42). Pathological overexpression of HSP27 has been reported in a wide spectrum of malignancies, which was associated with poor prognosis in different types of tumors, including high grade invasive gliomas. Correlation analysis on HSP27 expression and tumor growth rate of astrocytomas revealed that abnormal levels of HSP27 were likely to promote tumor growth (18). It has also been reported that the majority of cells in a given GBM mass could be generated by a very small fraction of self-renewing, multipotent tumor initiating cells/cancer stem cells (CSCs) that may be accountable for tumor growth, recurrence, and resistance to chemo- and radiotherapies (5,11,25,35). Indeed, in addition to sustainable increases of HSP27, 38.5℃-cultured G55 transiently augmented CD133 expression in a small subpopulation. CD133 (i.e., prominin-1) is a glycoprotein that in humans is encoded by the PROM1 gene that has been considered as a representative marker of CSCs (5,11,44). Thus, our results that rats received 38.5℃ preconditioned G55 demonstrated more aggressively developing tumors that were less sensitivity to 5-FU treatment, suggest that milder heat stress exposures may induce transiently increased expression of CD133 in a fraction of glioma cells that may be more resilient for

CT-1573 Cell Transplantation early e-pub; provisional acceptance 04/29/2016

survival and proliferation (e.g., as per our *in vitro* data, none of the CD133 positive G55 cells exhibited cleaved caspase-3, an apoptotic marker following bolus 5-FU treatment). Lately, analyses based on bench data and mathematical modeling indicated a possibility that stem cell-like tumor initiation cells may not be a fixed population; instead, expressions of CSC markers may likely transient oncological events occurring in a selected population of cancer cells when induced by environmental and genetic impacts (26,27). We are currently exploring whether mild hyperthermia-stressed glioma cells also have constitutively activated HSP27 in CD133+ cells as reported before for CSCs under hypoxia and serum depletion to inhibit caspase activation (22). Although hyperthermia therapy has been conventionally reasoned as a putative treatment for different types of malignant tumors including GBM, data from large size controlled studies remains lacking (40). Noticeably, fever is one of the most common signs for the initial diagnosis and in the terminal stage of GBM patients (38). Therefore, systematical studies will be needed to examine potential oncogenic modifying or enhancing effect of hyperthermia regimens on glioma and other types of cancer cells through applying stem cell biology-oriented designs (25,26).

We recently reported that genetically engineered human neural stem cells plus prodrugs efficaciously treated glioblastoma in the first rat model of ISCG manifesting both somatomotor and autonomic abnormalities (30). The present study has, in addition, established an effective approach of thermal precondition of human high grade glioma cells for alternating their oncological features *in vitro* and *in vivo*. Using the mild thermal exposure tactic, we have developed a protocol of manipulating growth dynamics of human glioma cells in the adult rat spinal cord. Taken together, our work provides new experimental systems for investigating oncogenic mechanisms and screening for potential oncolytic therapeutics to treat spinal cord malignant tumors. The findings may additionally facilitate future investigations of hyperthermia

CT-1573 Cell Transplantation early e-pub; provisional acceptance 04/29/2016

impact on malignant tumor cells and therapeutic discoveries for currently intractable metastatic diseases.

Acknowledgements

This work was supported by Teng Lab Research Fund, CASIS-NASA, and SCIRP-DoD grants to Y.D.T., and a grant to Y.D.T. & R.D.Z. from the Cele H. & William B. Rubin Family Fund, Inc. for the Gordon Program in Clinical Paralysis Research. We thank Dr. E.Y. Snyder of SBPDC for providing G55 cells. X.Z., I.B.H., M.A., Z.A., J.E.A., and Y.D.T. undertook major experimentation plus data processing. X.Z., I.B.H., and M.A. contributed to the study design refinement. R.D.Z. and J.H.C. provided partial grant support and advice for the study design and data analysis. X.Z. and Y.D.T. drafted the manuscript. Y.D.T. conceived and designed the study, provided funding, supervised all experimentation, performed data analyses, and wrote and finalized the paper. The authors declare that they have no competing financial interests for the reported project.

The authors declare no conflicts of interest.

References

1. Glossary of terms for thermal physiology. Second edition. Revised by The Commission for Thermal Physiology of the International Union of Physiological Sciences (IUPS Thermal Commission). Pflugers Arch 410(4-5):567-587; 1987.

2. Abrams, R.; Hammel, H. T. Hypothalamic Temperature in Unanesthetized Albino Rats during Feeding and Sleeping. Am. J. Physiol. 206:641-646; 1964.

3. Arrigo, A. P. In search of the molecular mechanism by which small stress proteins counteract apoptosis during cellular differentiation. J Cell Biochem 94(2):241-246; 2005.

4. Arya, R.; Mallik, M.; Lakhotia, S. C. Heat shock genes - integrating cell survival and death. J. Biosci. 32(3):595-610; 2007.

5. Bao, S.; Wu, Q.; McLendon, R. E.; Hao, Y.; Shi, Q.; Hjelmeland, A. B.; Dewhirst, M. W.; Bigner, D. D.; Rich, J. N. Glioma stem cells promote radioresistance by preferential activation of the DNA damage response. Nature 444(7120):756-760; 2006.

6. Basso, D. M.; Beattie, M. S.; Bresnahan, J. C. A sensitive and reliable locomotor rating scale for open field testing in rats. J. neurotrauma 12(1):1-21; 1995.

7. Bouchentouf, M.; Benabdallah, B. F.; Tremblay, J. P. Myoblast survival enhancement and transplantation success improvement by heat-shock treatment in mdx mice. Transplantation 77(9):1349-1356; 2004.

8. Caplan, J.; Pradilla, G.; Hdeib, A.; Tyler, B. M.; Legnani, F. G.; Bagley, C. A.; Brem, H.; Jallo, G. A novel model of intramedullary spinal cord tumors in rats: functional progression and histopathological characterization. Neurosurgery 59(1):193-200; discussion 193-200; 2006.

9. Concannon, C. G.; Gorman, A. M.; Samali, A. On the role of Hsp27 in regulating apoptosis. Apoptosis 8(1):61-70; 2003.

10. Drela, K.; Sarnowska, A.; Siedlecka, P.; Szablowska-Gadomska, I.; Wielgos, M.; Jurga, M.; Lukomska, B.; Domanska-Janik, K. Low oxygen atmosphere facilitates proliferation and maintains undifferentiated state of umbilical cord mesenchymal stem cells in an hypoxia inducible factor-dependent manner. Cytotherapy 16(7):881-892; 2014.

11. Galli, R.; Binda, E.; Orfanelli, U.; Cipelletti, B.; Gritti, A.; De Vitis, S.; Fiocco, R.; Foroni, C.; Dimeco, F.; Vescovi, A. Isolation and characterization of tumorigenic, stem-like neural precursors from human glioblastoma. Cancer Res. 64(19):7011-7021; 2004.

12. Fidler, I.J. The organ microenvironment and cancer metastasis. Differentiation. 70(9-10):498-505; 2002.

13. Garrido, C.; Brunet, M.; Didelot, C.; Zermati, Y.; Schmitt, E.; Kroemer, G. Heat shock proteins 27 and 70: anti-apoptotic proteins with tumorigenic properties. Cell Cycle 5(22):2592-2601; 2006.

14. Hsu, S.; Quattrone, M.; Ostrom, Q.; Ryken, T. C.; Sloan, A. E.; Barnholtz-Sloan, J. S. Incidence patterns for primary malignant spinal cord gliomas: a Surveillance, Epidemiology, and End Results study. J. Neurosurg. Spine 14(6):742-747; 2011.

15. Hsu, W.; Siu, I. M.; Pradilla, G.; Gokaslan, Z. L.; Jallo, G. I.; Gallia, G. L. Animal model of intramedullary spinal cord glioma using human glioblastoma multiforme neurospheres. J. Neurosurg. Spine 16(3):315-319; 2012.

16. Ito, M.; Ohba, S.; Gaensler, K.; Ronen, S.M.; Mukherjee, J.; Pieper, R.O. Early Chk1 phosphorylation is driven by temozolomide-induced, DNA double strand break- and mismatch repair-independent DNA damage. PLoS One 8(5): e62351; 2013.

17. Ju, D.; Yamaguchi, F.; Zhan, G.; Higuchi, T.; Asakura, T. et al. Hyperthermotherapy enhances antitumor effect of 5-aminolevulinic acid-mediated sonodynamic therapy with activation of caspase-dependent apoptotic pathway in human glioma. Tumour Biol. 2016 Feb 4. [Epub ahead of print]

18. Khalid, H.; Tsutsumi, K.; Yamashita, H.; Kishikawa, M.; Yasunaga, A.; Shibata, S. Expression of the small heat shock protein (hsp) 27 in human astrocytomas correlates with histologic grades and tumor growth fractions. Cell Mol. Neurobiol. 15(2):257-268; 1995.

19. Kim, H.; Cooke, M. J.; Shoichet, M. S. Creating permissive microenvironments for stem cell transplantation into the central nervous system. Trends Biotechnol. 30(1):55-63; 2012.

20. Kim, K.J.; Li, B.; Winer, J; Armanini, M.; Gillett, N.; Phillips, H.S.; Ferrara, N. Inhibition of vascular endothelial growth factor-induced angiogenesis suppresses tumor growth in vivo. Nature 362:841-844; 1993.

21. Komata, T.; Kanzawa, T.; Nashimoto, T.; Aoki, H.; Endo, S.; Nameta, M.; Takahashi, H.; Yamamoto, T.; Kondo, S.; Tanaka, R. Mild heat shock induces autophagic growth arrest, but not apoptosis in U251-MG and U87-MG human malignant glioma cells. J. Neurooncol. 68(2):101-111; 2004.

22. Lin, S.P.; Lee, Y.T.; Wang, J.Y.; Miller, S.A.; Chiou, S.H.; Hung, M.C.; Hung, S.C. Survival of cancer stem cells under hypoxia and serum depletion via decrease in PP2A activity and activation of p38-MAPKAPK2-Hsp27. PLoS One. 7(11):e49605; 2012.

23. Matsumoto, T.; Urasaki, E.; Soejima, Y.; Nakano, Y.; Yokota, A.; Nishizawa, S. Cervical intramedullary glioblastoma: report of a long-term survival case and a review of the literature. J. Uoeh 30(4):413-420; 2008.

24. Motaln, H.; Koren, A.; Gruden, K.; Ramšak, Ž.; Schichor, C.; Lah, TT. Heterogeneous glioblastoma cell cross-talk promotes phenotype alterations and enhanced drug resistance. Oncotarget 6(38):40998-41017; 2015.

25. Munoz, J. L.; Rodriguez-Cruz, V.; Greco, S. J.; Ramkissoon, S. H.; Ligon, K. L.; Rameshwar, P. Temozolomide resistance in glioblastoma cells occurs partly through epidermal growth factor receptor-mediated induction of connexin 43. Cell Death Dis. 5:e1145; 2014.

26. Pillat, M. M.; Oliveira, M. N.; Motaln, H.; Breznik, B.; Glaser, T.; Lah, T. T.; Ulrich, H. Glioblastoma-mesenchymal stem cell communication modulates expression patterns of kinin receptors: Possible involvement of bradykinin in information flow. Cytometry A; 2015.

27. Poleszczuk, J.; Enderling, H. Cancer Stem Cell Plasticity as Tumor Growth Promoter and Catalyst of Population Collapse. Stem Cells Int. 2016:3923527; 2016.

28. Poleszczuk, J.; Hahnfeldt, P.; Enderling, H. Evolution and phenotypic selection of cancer stem cells. PLoS Comput Biol. 11(3):e1004025; 2015

29. Rajan, A.; Eubanks, E.; Edwards, S.; Aronovich, S.; Travan, S.; Rudek, I.; Wang, F.; Lanis, A.; Kaigler, D. Optimized cell survival and seeding efficiency for craniofacial tissue engineering using clinical stem cell therapy. Stem Cells Transl. Med. 3(12):1495-1503; 2014.

30. Ropper, A. E.; Zeng, X.; Haragopal, H.; Anderson, J. E.; Aljuboori, Z.; Han, I.; Abd-El-Barr, M.; Lee, H. J.; Sidman, R. L.; Snyder, E. Y. and others. Targeted Treatment of Experimental Spinal Cord Glioma With Dual Gene-Engineered Human Neural Stem Cells. Neurosurgery; 2015.

31. Rubenstein, J.L.; Kim, J.; Ozawa, T.; Zhang, M.; Westphal, M.; Deen, D.F.; Shuman, M.A. Anti-VEGF antibody treatment of glioblastoma prolongs survival but results in increased vascular cooption. Neoplasia 2(4):306-314; 2000.

32. Samali, A.; Holmberg, C. I.; Sistonen, L.; Orrenius, S. Thermotolerance and cell death are distinct cellular responses to stress: dependence on heat shock proteins. FEBS Lett. 461(3):306-310; 1999.

33. Samartzis, D.; Gillis, C. C.; Shih, P.; O'Toole, J. E.; Fessler, R. G. Intramedullary Spinal Cord Tumors: Part I-Epidemiology, Pathophysiology, and Diagnosis. Global Spine J. 5(5):425-435; 2015.

34. Seidel, S.; Garvalov, B.K.; Wirta, V.; von Stechow, L.; Schänzer, A. et al. A hypoxic niche regulates glioblastoma stem cells through hypoxia inducible factor 2 alpha. Brain 133(Pt 4):983-995; 2010.

35. Singh, S. K.; Hawkins, C.; Clarke, I. D.; Squire, J. A.; Bayani, J.; Hide, T.; Henkelman, R. M.; Cusimano, M. D.; Dirks, P. B. Identification of human brain tumour initiating cells. Nature 432(7015):396-401; 2004.

36. Spencer, F.; Shirer, H. W.; Yochim, J. M. Core temperature in the female rat: effect of pinealectomy or altered lighting. Am. J. Physiol. 231(2):355-360; 1976.

37. Su, C. Y.; Chong, K. Y.; Chen, J.; Ryter, S.; Khardori, R.; Lai, C. C. A physiologically relevant hyperthermia selectively activates constitutive hsp70 in H9c2 cardiac myoblasts and confers oxidative protection. J. Mol. Cell Cardiol. 31(4):845-855; 1999.

38. Teng, Y. D.; Wrathall, J. R. Evaluation of cardiorespiratory parameters in rats after spinal cord trauma and treatment with NBQX, an antagonist of excitatory amino acid receptors. Neurosci. Lett. 209(1):5-8; 1996.

39. Their, K.; Calabek, B.; Tinchon, A.; Grisold, W.; Oberndorfer, S. The last 10 days of patients with glioblastoma: assessment of clinical signs and symptoms as well as treatment. Am. J. Hosp. Palliat. Care 2015 [Epub ahead of print]

40. Titsworth, W.L.; Murad G.J.; Hoh, B.L.; Rahman, M. Fighting fire with fire: the revival of thermotherapy for gliomas. Anticancer Res. 34(2):565-574; 2014.

41. Voll, E. A.; Ogden, I. M.; Pavese, J. M.; Huang, X.; Xu, L.; Jovanovic, B. D.; Bergan, R. C. Heat shock protein 27 regulates human prostate cancer cell motility and metastatic progression. Oncotarget 5(9):2648-2663; 2014.

42. Wang, X.; Chen, M.; Zhou, J.; Zhang, X. HSP27, 70 and 90, anti-apoptotic proteins, in clinical cancer therapy (Review). Int. J. Oncol. 45(1):18-30; 2014.

43. Westphal, M.; Hansel, M.; Hamel, W.; Kunzmann, R.; Holzel, F. Karyotype analyses of 20 human glioma cell lines. Acta Neurochir (Wien) 126:17-26; 1994.

44. Wu, B.; Sun, C.; Feng, F.; Ge, M.; Xia, L. Do relevant markers of cancer stem cells CD133 and Nestin indicate a poor prognosis in glioma patients? A systematic review and meta-analysis. J. Exp. Clin. Cancer Res. 34:44; 2015.

45. Yu, D.; Thakor, D. K.; Han, I.; Ropper, A. E.; Haragopal, H.; Sidman, R. L.; Zafonte, R.; Schachter, S. C.; Teng, Y. D. Alleviation of chronic pain following rat spinal cord

compression injury with multimodal actions of huperzine A. Proc. Natl. Acad. Sci. U S A 110(8):E746-755; 2013.

46. Zolzer, F.; Streffer, C. Quiescence in S-phase and G1 arrest induced by irradiation and/or hyperthermia in six human tumour cell lines of different p53 status. Int. J. Radiat. Biol. 76(5):717-725; 2000.

Figure legends

Figure 1. Promotion of glioma cell growth *in vitro* by mild hyperthermia

U87 and G55 glioblastoma cells showed significantly augmented cell proliferation rate when cultured in 38.5°C ambient condition for 1-2 passages (i.e., P1 and P2). Group average cell doubling time (CDT), relative to P0 baseline values, was significantly shortened in U87 (e.g., from P0 CDT of 21.55 ± 0.13 hours to P2 CDT of 20.40 ± 0.32 hours, n = 9, $P < 0.05$, One-way ANOVA with Tukey HSD test) and in G55 cells (e.g., from P0 CDT of 19.31 ± 0.11 to P2 CDT of 17.40 ± 0.37 hours, n = 9, $P < 0.05$, One-way ANOVA with Tukey HSD test).

Figure 2. Upregulation of HSP27 expression in glioma cells following 38.5°C precondition

Under 37.0°C culture, about 7.41 ± 2.23% of G55 cells showed immunoreactivity for heat shock protein 27 kDa (HSP27) (**A**). By contrast, when the cells were cultured in 38.5°C (P0), % of cells immunopositive for HSP27 increased significantly to 72.52 ± 1.77% (n = 9, $P < 0.05$, One-way ANOVA with Tukey HSD test) (**B**). However, when G55 cells were continuously cultured in 38.5°C for 3 passages (P2: ~9 days), the percentage of HSP27 immunopositive cells reduced to 60.33 ± 2.28% (n = 9, $P < 0.05$, One-way ANOVA with Tukey HSD test) (**C**). A summary of % of HSP27 immunopositive cells in different groups was presented in **D**. Insets: Typical density of DAPI-labeled nuclei of ~80% confluent cells that were cultured under different temperatures. Percentage of HSP27 ICC positive cells were quantified via dividing the total HSP27 immunopositive cell number by the total number of DAPI labeled nuclei under each randomly sampled area (see Methods for details). Scale bar = 10 μm. * indicates $P < 0.05$ compared to cells in 37°C culture condition, # indicates $P < 0.05$ compared to P0 cells in 38.5°C culture condition.

CT-1573 Cell Transplantation early e-pub; provisional acceptance 04/29/2016

Figure 3. Culture of 38.5°C transiently elevated CD133 expression in a G55 subpopulation but did not trigger caspase-3 cleavage in those cells

In 37.0°C setting, 2.7 ± 0.16% of G55 cells expressed CD133. However, CD133 expression percentage of 38.5°C-cultured P0 G55 increased to 6.48 ± 0.36 but subsequently reduced to 3.96 ± 0.13 in P2 cells, showing a transient pattern though the latter remaining significantly higher than control level ($P < 0.05$, n = 15/group, ANOVA with Tukey HSD test; **Figure 3A-D**). Following 38.5°C culture, there was a significantly increased rate of apoptosis in G55 P0 cells but the degree of increase was very limited (i.e., 2.34 ± 0.13% vs. 1.64 ± 0.16% of 37.0°C; $P < 0.05$, n = 15/group, ANOVA with Tukey HSD test; **Figure 3E-H**) as detected by nuclear presence of cleaved caspase-3 (see details in orthoslice images in the larger inset). The apoptotic cell percentage decreased to 1.56 ± 0.10% in 38.5°C P2 cells that was insignificant comparing to 37.0°C control cells (1.64 ± 0.16%). In all the settings, immunoreactivity to cleaved caspase-3 was only observed in G55 cells that were negative for CD133 expression (**Figure 3E-G**; note: A-D respectively showed the same imaging fields of E-G). The total cell number estimates were presented in **D** and **H**. Insets: Typical density of DAPI-labeled nuclei of ~70-80% confluent cells that were cultured under different temperatures.

Figure 4. *In vivo* oncological profile of G55 post 38.5°C precondition in the spinal cord

Implantation of 38.5°C preconditioned G55 cells resulted in significantly larger outgrowth of the tumor compared with that derived from 37.0°C precultured G55 at C2 and T10 spinal cord as measured by the length and width of the glioma mass (**A**). As a physical sign of tumor progress, rats showed gradual impairment of the hind limb locomotor function and eventually lost their

CT-1573 Cell Transplantation early e-pub; provisional acceptance 04/29/2016

capability to sustain performing body weight-bearing stepping (i.e. BBB score ≤9). This was the time when intratumor 5-fluorouracil (5-FU; dose: 0.1 micromole) was administered to assess sensitivity to chemotherapy (i.e., oncological aggressiveness). Rats with 38.5°C preconditioned G55 implant at either C2 or T10 had very poor response to bolus 5-FU treatment, showing continued deterioration of BBB scores 72 hours later; by contrast, rats with 37.0°C cultured G55 responded well to the treatment, with their BBB scores being maintained at similar levels showing slight improvement (**B**). In fact, the group individual BBB score change (i.e., BBB at the day of 5-FU injection – BBB at 72 hours post 5-FU) in average was 3.33 ± 0.42 of the 38.5°C group versus -1.33 ± 0.92 for the 37.0°C group ($P < 0.01$, n = 6/group, paired Student's *t*-test) (**C**, right column). The data suggested that 38.5°C precondition made G55 cells more malignant. The notion was validated by rat post-tumor survival evaluation. Specifically, rats with 38.5°C preconditioned G55 cells in C2 or T10 spinal cord showed a group mean survival of 15.33 ± 0.67 days post G55 transplantation, which was significantly shorter than rats received 37.0°C precultured G55 (18.33 ± 0.71 days, n = 6/group, $P = 0.012$, unpaired Student's *t* test) (**C**, left column). * indicates $P < 0.05$ when compared to rats receiving 37°C precultured G55.

Figure 5. Pathological features of thermal preconditioned G55 glioma in the spinal cord

Five out of the six spinal cords showed dorsal surface disruption by the outgrowth of glioma mass derived from the implanted G55 cells following 38.5°C precondition (upper row). By contrast, none of the tumors derived from 37.0°C preconditioned G55 grew above the dorsal surface in the six spinal cords (lower row). **Right**: H&E stain demonstrated representative pathological scale of the intramedullary growth of the glioma mass for each group.

CT-1573 Cell Transplantation early e-pub; provisional acceptance 04/29/2016

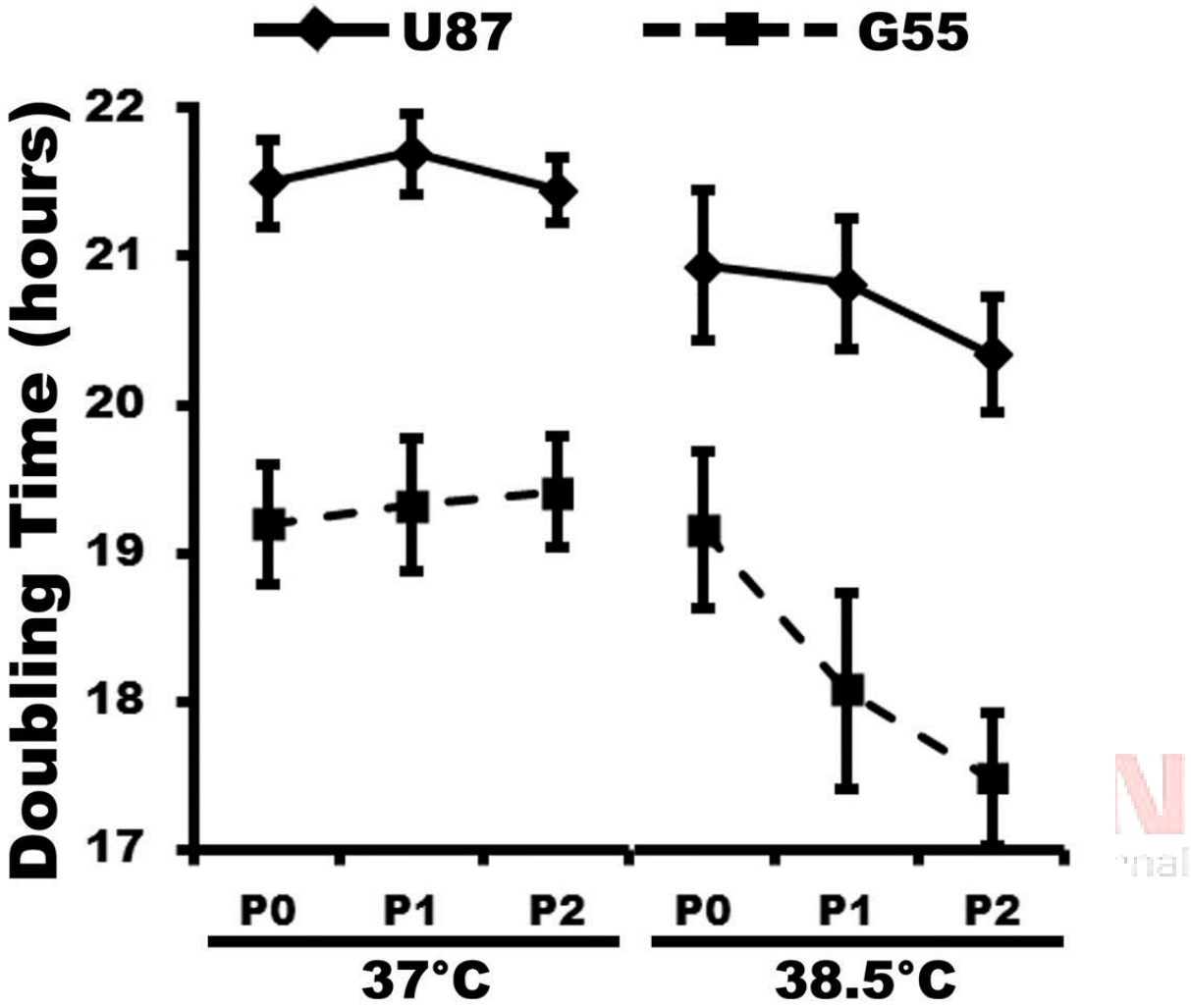

Figure 1

CT-1573 Cell Transplantation early e-pub; provisional acceptance 04/29/2016

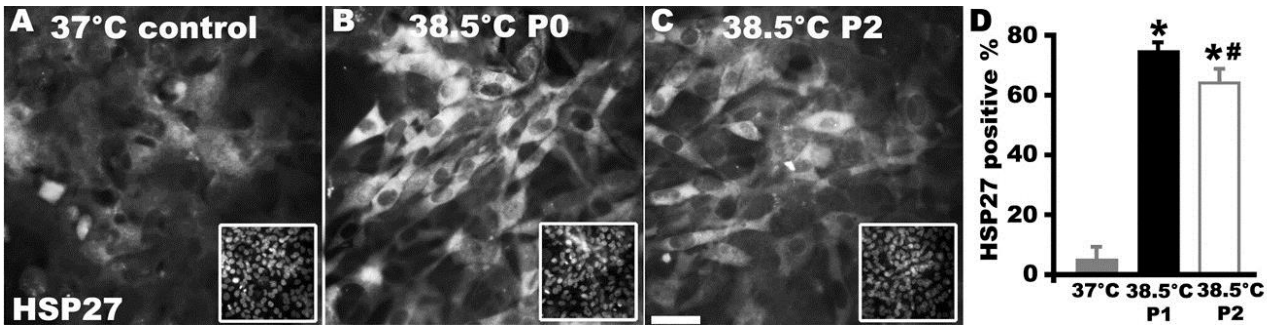

Figure 2

CT-1573 Cell Transplantation early e-pub; provisional acceptance 04/29/2016

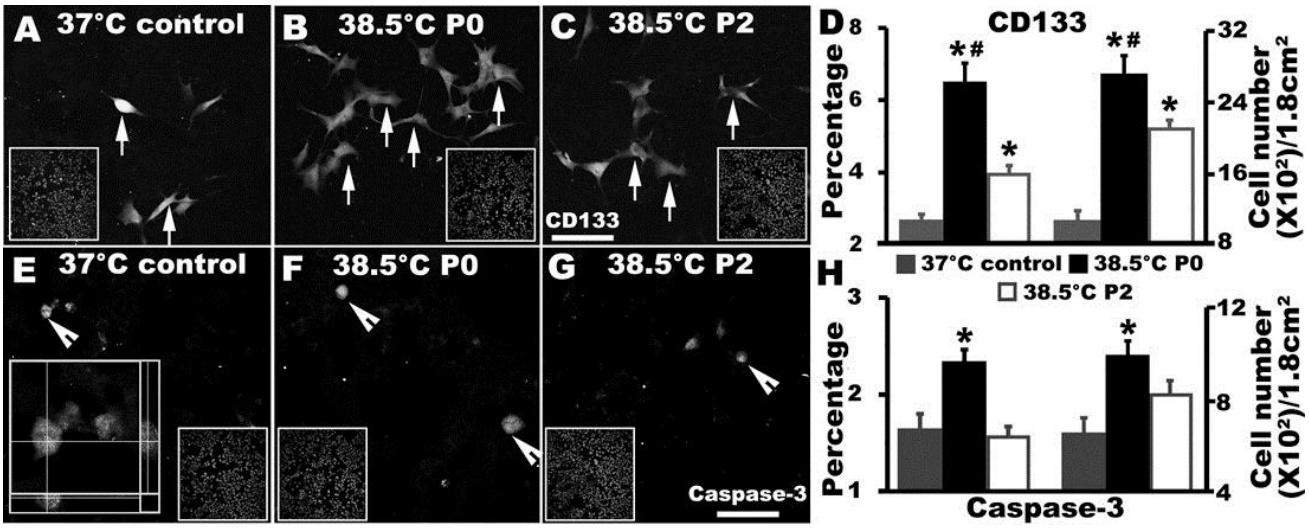

Figure 3

CT-1573 Cell Transplantation early e-pub; provisional acceptance 04/29/2016

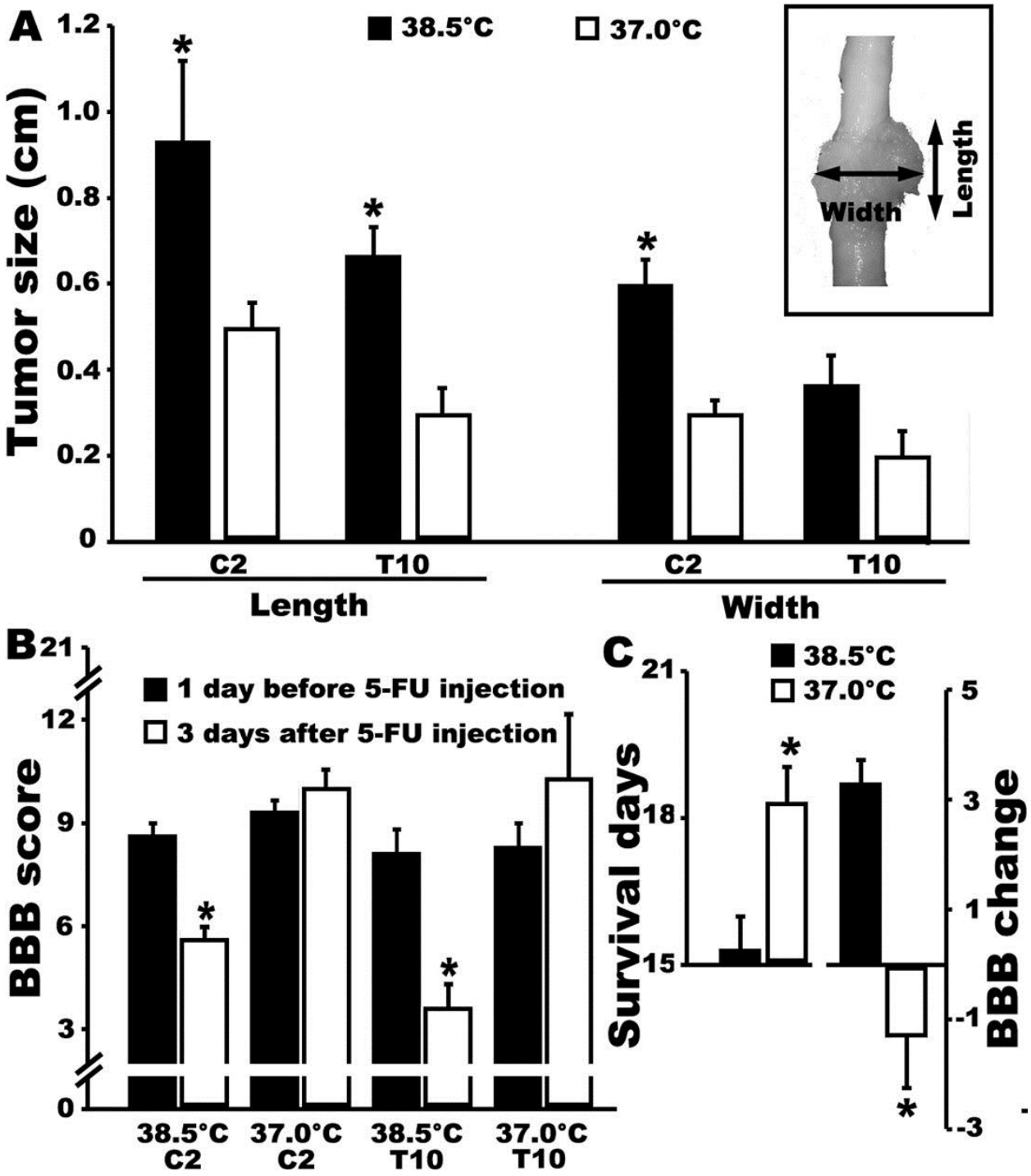

Figure 4

CT-1573 Cell Transplantation early e-pub; provisional acceptance 04/29/2016

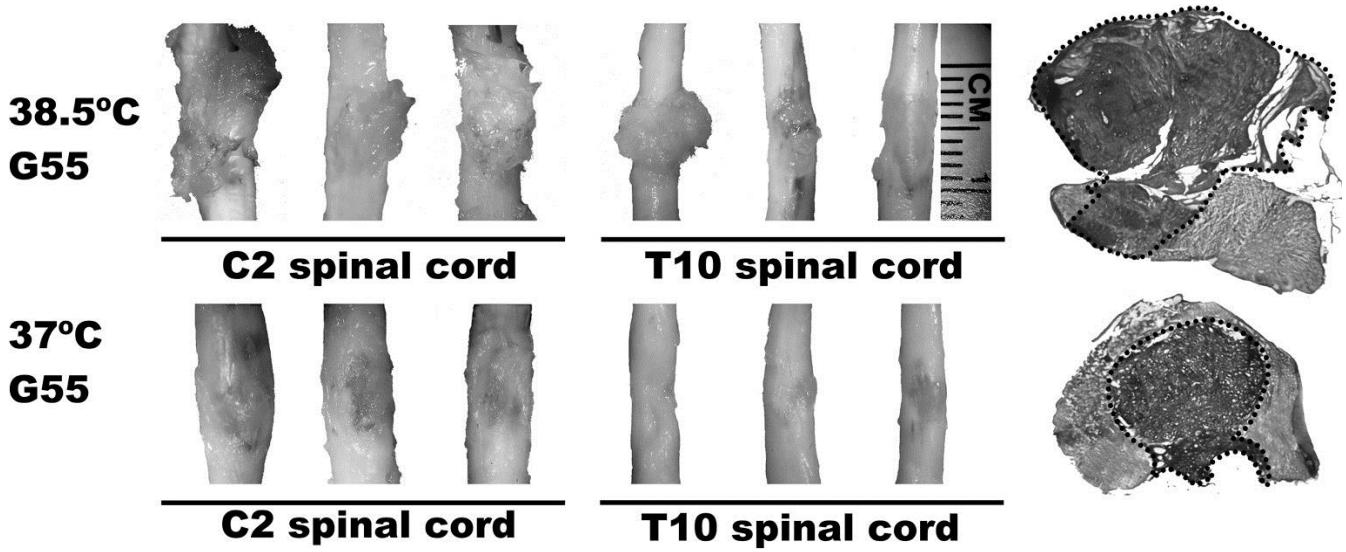

Figure 5

CT-1573 Cell Transplantation early e-pub; provisional acceptance 04/29/2016

Table 1. *In vivo* profiles of G55 growth and response to 5-FU treatment after intraspinal cord implantation

ID	Thermal condition & tumor site	Tumor length (cm)	Tumor width (cm)	Tumor outgrowth	The first daily BBB drop to ≤9 (unit: score)	BBB scale at 72 h after 5-FU injection (unit: score)	Survival duration (first daily BBB ≤9) (unit: day)
1	38.5 °C G55, C2	1.3	0.7	Dorsal dura disruption	9	6	15
7	38.5 °C G55, C2	0.7	0.5	Dorsal dura disruption	8	6	13
9	38.5 °C G55, C2	0.8	0.6	Dorsal dura disruption	9	5	16
8	38.5 °C G55,T10	0.6	0.5	Dorsal dura disruption	6	3	15
10	38.5 °C G55,T10	0.6	0.3	Dorsal disruption	8	5	17
12	38.5 C G55,T10	0.8	0.3	Inside spinal cord	8	3	14
2	37°C G55, C2	0.6	0.3	Inside spinal cord	10	9	18
5	37°C G55, C2	0.5	0.3	Inside spinal cord	9	11	19
11	37°C G55, C2	0.4	0.3	Inside spinal cord	9	10	16
3	37°C G55,T10	0.2	0.1	Inside spinal cord	7	9	17
4	37°C G55,T10	0.3	0.2	Inside spinal cord	9	14	19
6	37°C G55,T10	0.4	0.3	Inside spinal cord	9	8	21

CT-1573 Cell Transplantation early e-pub; provisional acceptance 04/29/2016